Accepted Manuscript online: 2022-08-17 Article published online: 2022-09-20

2,5-Diaryl 6-hydroxyphenalenones for Single-Molecule Junctions

David Vogel*[a]
Luca Ornago[b]
Christina Wegeberg[a]
Alessandro Prescimone[a]
Herre van der Zant[b]
Marcel Mayor*[a,c,d]

[a] Department of Chemistry, University of Basel, St. Johanns-Ring 19, CH-4056 Basel, Switzerland
[b] Kavli Institute of Nanoscience, Delft University of Technology, Lorentzweg 1, 2628 CJ Delft, The Netherlands
[c] Institute for Nanotechnology (INT), Karlsruhe Institute of Technology (KIT), P.O. Box 3640, 76021 Karlsruhe, Germany
[d] Lehn Institute of Functional Materials, School of Chemistry, Sun Yat-Sen University, Guangzhou 510274, P.R. of China
* david.vogel@unibas.ch; marcel.mayor@unibas.ch

Received: 30.06.2022
Accepted after revision: 12.08.2022
DOI: 10.1055/a-1926-6340; Art ID: OM-2022-06-0015-OA

Abstract A modular access to 2,5-diaryl 6-hydroxyphenalenone derivatives is developed and demonstrated by a small series of 5 molecules. Within this series, the structures **1** and **2** expose terminal methylsulfanyl anchor groups, enabling their integration in a single-molecule junction. The modular synthesis is based on Suzuki cross-coupling of the aryl substituents as boronic acid precursors with 5,8-dibromo-2-(*tert*-butyl)-4,9-dimethoxy-2,3-dihydro-1H-phenalen-1-one, and the subsequent transformation of the product to the desired 2,5-diaryl 6-hydroxyphenalenone in a reduction/deprotection sequence. The new structures are fully characterized and their optical and electrochemical properties are analysed. For the derivatives **1** and **2** suitable for single-molecule junctions, the corresponding oxophenalenoxyl radicals **1R** and **2R** were obtained by oxidation and analysed by electron paramagnetic resonance spectroscopy. Preliminary mechanical break junction experiments with **1** display the structure's ability to form transient single-molecule junctions. The intention behind the molecular design is to profit from the various redox states of the structure (including the neutral radical) as a molecular switch in an electrochemically triggered single-molecule transport experiment.

Key words: oxophenalenoxyl radicals, 6-hydroxyphenalenone, molecular switches, voltammetry, organic chemistry, molecular break junctions

Introduction

Over the last decades, the employed components in electronics have been continuously downsized. Following this miniaturisation trend, which was predicted by Moore's Law,[1] the semiconductor industry is constantly looking for novel concepts allowing for further miniaturisation. A promising concept is single-molecule electronics. Molecules are the smallest known object with enough structural diversity to integrate a particular function by structural design. Supported by the continuously growing skills in synthetic chemistry, the variety of such single molecular devices is increasing steadily. Examples of electronic functions that were realized following this bottom-up approach are information storage,[2–4] transistors,[5–7] diodes,[8,9] switches,[9–13] sensors,[14] and translation of an electric field into mechanical movement,[15] to name a few. Molecules being able to switch between several different metastable states are of fundamental interest as potential gate openers towards electronic concepts beyond the current binary technology.[16–18]

Molecular switches require at least two moderately stable states. The different states have to be stable enough that a switched molecule remains in the respective state if no external stimulus is given but reactive enough that a mild external stimulus may convert them into another state.[13] It is of great importance that the switching mechanism is of reversible nature and results in quantitative conversion. There are in general two different types of molecular switches: conformational and/or redox switches. The first type is switched by a structural change, for example, breaking a bond,[19–22] while the latter is switched by moving from one oxidation state to another, as for example from an uncharged molecule to an anion or a cation.[23–25] Several different external stimuli have been reported, such as current-induced switching, redox-potential-induced switching,[26–28] field-induced switching,[26,29] light-induced switching,[30] thermal-induced switching[31–33] and stretching-induced switching.[34] To detect the switching event, an externally observable molecular property has to be altered.

Single-molecule electronic or thermal transport properties and the related logical functions are most often investigated using molecular break junction (MBJ) experiments.

There are two main types of MBJs employed for the investigation of these phenomena.

A scanning tunnelling microscope (STM) can be employed to investigate molecules deposited on a surface by probing them between the cantilever tip of the STM and the surface.[35–37] While the experiment allows investigation of the substrate and selection of particular promising molecular candidates, the molecular junction is formed between two very different electrodes. A more symmetrical metal–molecule–metal junction is realized in a mechanically controlled break junction (MCBJ) experiment.[37–39] Integrating the molecule of interest between the electrodes of either system often increases the constraints to the switchable system. For example, the exciton formed on a photoswitchable molecule upon illumination might diffuse into the electrodes quicker than the molecular switching event takes place. Also conformational rearrangements in a switching process might be sterically handicapped by the proximity of the electrodes.[13]

The amount of metastable states accessible by a molecule correlates directly with the amount of operations a molecular switch is able to perform. The majority of molecular switches reported so far are mainly able to access two different molecular states and thus are limited to binary operations.[40–45] Extending the amount of metastable states accessible by an external stimulus from two to more, e.g. three, would therefore be highly desirable. Only very few examples of three-state switches have been reported, like, e.g., a naphthalene diimide (NDI) switch.[46] The latter example served as inspiration for the here-reported molecular design based on 6-hydroxyphenalenone derivatives. We hypothesized that the improved stability of oxophenalenoxyl radicals compared to NDI radicals should ease their handling. Additionally, the anion of the 6-hydroxyphenalenone should be easily accessible not only electrochemically, but also by conventional wet chemical treatment as already reported for the acid/base switch by Ratner et al.[14] Consequently, two switching processes are expected for the here-represented 6-hydroxyphenalenone derivatives. In an electrochemically controlled single-molecule transport experiment, both processes should be accessible, i.e. the formation of the radical by oxidation as well as the formation of the anion by reduction of the parent structure. Interestingly, switching between the anionic and the neutral form is also achievable by pH variation.

Here a synthetic route to 2,5-diaryl 6-hydroxyphenalenones is developed and documented with a variety of derivatives (**1**–**5**, Figure 1A), including the model compounds **1** and **2** exposing methyl-sulfide anchoring groups at the *para*-position of the aryl substituents as derivatives suited for single-molecule transport experiments. While the switching of the 6-hydroxyphenalenone derivatives is mainly investigated in solution, preliminary MCBJ experiments show that single-molecule junctions can be obtained from **1**.

Results and Discussion

Molecular Design and Switching Concept

6-Hydroxyphenalenone derivatives are particularly appealing model compounds for single-molecule junctions. The over the entire core delocalized π-system remains stable in a variety of redox states. As a result, electrochemically induced state switching events should lead to substantial transport differences in single-molecule junctions not clouded by the degradation of the oxidized or reduced derivatives. While such a set-up resembles the already men-

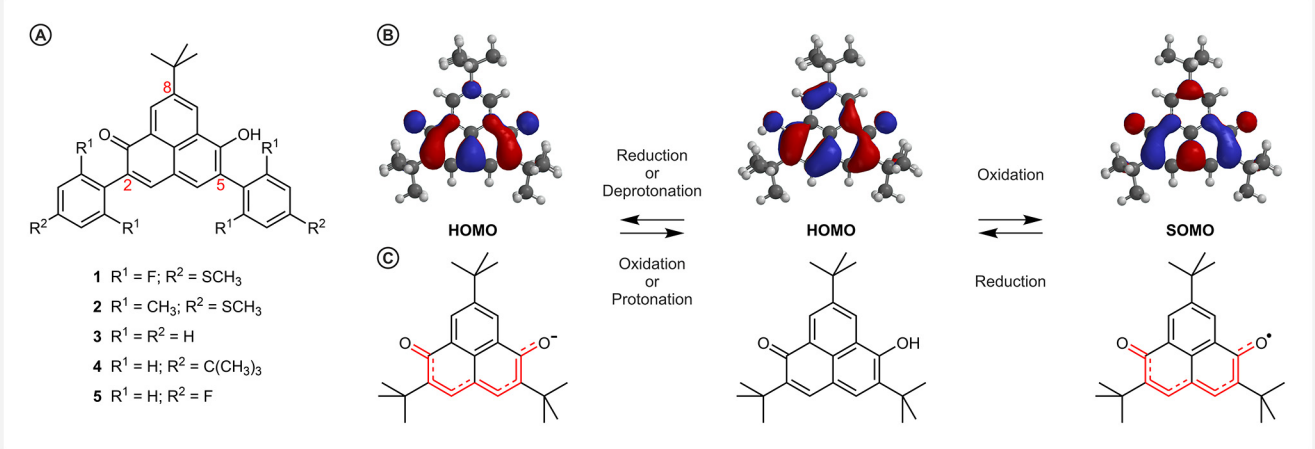

Figure 1 **A)** Molecular structures of 2,5-diaryl 6-hydroxyphenalenones **1**–**5**. **B)** Calculated electron density maps of the populated frontier orbitals of 2,5,8-tri-tert-butyl 6-hydroxyphenalenone (centre) and its corresponding anion (left) and oxophenalenoxyl radical (right). **C)** Molecular structures corresponding to the electron density maps depicted in **A)**.

tioned single NDI junction,[46] the even more desirable properties of 6-hydroxyphenalenone-based model compounds are their relatively stable radical forms. Immobilized in a molecular junction, the interaction of the transport current with the unpaired electron will be the focus of interest. In order to optimize the target structure for future single-molecule transport experiments, the different metastable states of 2,5-diaryl 6-hydroxyphenalenones are studied in solution and their properties are evaluated as proxy for future investigations in molecular junctions.

In the first papers about oxophenalenoxyl radical derivatives, Nakasuji et al reported in 1996 that their lability did not allow their isolation.[47,48] However, since the year 2000, a variety of derivatives have been reported with stability features allowing their isolation.[49–55] The common structural feature of all these isolated derivatives are *tert*-butyl groups at their 2- and 5-positions. The substituent at the 8-position has been varied from the parent hydrogen[49] to *tert*-butyl,[50] nitrile,[52] *para*-substituted phenyls,[51] and tetrathiafulvalene.[55] According to density functional theory calculations and previous experimental reports,[48,49,51,52] the highest spin density of the singly occupied molecular orbital (SOMO) is localized at positions 2 and 5 (Figure 1).

These are thus the most promising positions for the attachment of anchoring groups to investigate oxophenalenoxyl radicals in a single-molecule junction. As potential model compounds, we thus wondered about the synthetic accessibility of 2,5-diaryl 6-hydroxyphenalenones and the stability of the corresponding oxophenalenoxyl radical obtained upon oxidation. A modular synthetic approach to introduce aryl substituents at the 2- and 5-positions would not only allow to vary the electron density of the entire delocalized π-system, but also to decorate the structure with terminal anchoring groups. Particularly appealing is the symmetry of the 2,5-diaryl radical structure, as recent studies with less symmetric stable organic radicals displayed not only direct coupling of the radical to a particular electrode, but also the appearance of alternative parallel conduction pathways.[56,57] These background currents are troublesome as they might cloud conductance features and conductance variations originating from the population of the frontier orbitals in the different switching states. Therefore, it is important to avoid alternative conduction pathways. Calculated electron density maps (Figure 1 B) suggest for the radicals an increase in conjugation along the molecular structure, probably reflected in an increased electronic transparency compared to the protonated parent derivative. Interestingly, also for the anion, interesting properties are expected. The electron density calculations regarding the anion point at a considerable increase in cross-conjugation on both frontier orbitals (HOMO and LUMO) compared to the native 6-hydroxyphenalenone.

Both, the anion and the oxophenalenoxyl radical, shall be formed in situ immobilized inside the junction either by wet chemical or electrochemical means from the 6-hydroxyphenalenone derivative. Thus the model compounds **1** and **2** exposing terminal methyl-sulfide anchoring groups moved into the focus of interest. The anchoring groups are chemically robust and known to form transient molecular junctions with well-defined conductivity features. As the proposed 2,5-diaryl substituents are less sterically demanding than *tert*-butyl groups, the stability of the corresponding oxophenalenoxyl radicals had to be investigated. A small variety of aryl substituents were considered to develop the chemistry with less precious precursors and to provide model compounds to investigate spectroscopic properties of this new family of compounds. While with **1** and **2** the steric demand of the aryl substituents is varied, **3**–**5** differ mainly in the electron density on the aryl substituents. Interestingly, the reduced steric demand of the aryl substituents enables their coplanar arrangement with the oxophenalenoxyl core, contributing to the overall improved stability of the radical due to increased delocalization of the SOMO. Another stabilizing effect is expected from the electron deficiency of the fluorine-decorated aryl substituents of **1**.

The retrosynthetic approach to the 6-hydroxyphenalenone derivatives is displayed in Scheme 1. To maximise the modularity of the synthesis, the different aryl substituents shall be introduced as late as possible. As the carbonyl group of **C** shall be reduced under basic conditions, which are known to potentially trigger halogen dance reactions, the aryl groups will be introduced before the carbonyl reduction to avoid potential challenges. The assembly strategy follows

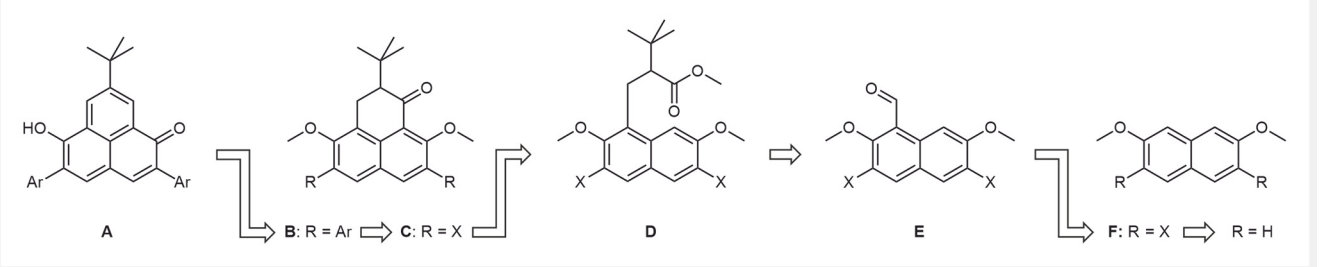

Scheme 1 Retrosynthetic approach towards the desired 6-hydroxyphenalenone derivatives (**A**) with aryl substituents at the 2- and 5-positions.

mainly the already reported syntheses of phenalenyl and oxophenalenoxyl derivatives.[49,51,53,58]

First, the 2,7-dihalo-3,6-dimethoxynaphthalene **F** shall be synthesized to provide the leaving groups for the subsequent introduction of the aryl substituents. Subsequent formylation provides **E**, which can be further developed into **D** by the addition of an enol ester followed by reductive removal of the benzylic hydroxyl group. The subsequent Friedel–Crafts ring closing reaction should provide **C**, as ideal precursor for the introduction of the various aryl substituents by Suzuki cross-coupling to yield **B**. Finally, reduction of the carbonyl followed by ether cleavage and aromatisation should give access to the targeted 6-hydroxyphenalenone derivatives.

Synthesis

The syntheses towards the key intermediate **14** were performed by adapting previously reported protocols for phenalenyl and oxophenalenoxyl derivatives (Scheme 2A).[49,51,53,58] The required 2,7-diboromo-3,6-dimethoxynaphthalene **8** was obtained by bromination of naphthalene-2,7-diole **6** in AcOH, followed by dehalogenation with tin in AcOH to afford **7**, which was further methylated with methyl iodide and potassium carbonate in acetone giving **8**. In our experiment, the literature-known 2,7-dibromo-3,6-dimethoxynaphthalene **8** was obtained in 78% yield over three steps.[59,60] A Rieche formylation with dichloromethyl methyl ether in the presence of $TiCl_4$ in DCM afforded the formylated naphthalene derivative **9** in 74% yield. Aldol addition of methyl *tert*-butylacetate to the formyl intermediate **9** using in situ prepared LDA in dry THF and subsequent reductive dehydroxylation yielded the methyl ester **11** in 86% yield over two steps. To our surprise, the saponification of the methyl ester **11** turned out to be challenging and the carboxylic acid **12** could only be obtained using harsh reaction conditions, which caused a considerable amounts of side products (Table S1). Also the subsequent Friedel–Crafts acylation with in situ formed acid chloride did not provide the targeted key intermediate **14**, but the demethylated derivative **15** instead.

To further disqualify this reaction sequence, all attempts to remethylate **15** failed (Table S2). As an alternative approach to **14**, the Friedel–Crafts type reaction reported between various alkyl esters and benzene promoted by triflic acid was considered and the protocol was adapted to our cyclisation.[61] And indeed, dissolving the methyl ester **11** in triflic acid yielded the desired key intermediate **14** in 91% yield. It was required to dissolve the methyl ester **11** in minimal DCM, if larger amounts than 100 mg of starting material were employed. Subsequent dropwise addition of this mixture to triflic acid yielded **14** in 86 ± 5% yield. As minor sideproduct, **13** was isolated, resulting from a halogen shift under these conditions. The observed halogen shift was surprising, as halogen dance reactions are usually reported for basic reaction conditions.[62] However, a few examples in acidic media are known too.[63] Purification of the triflic acid by

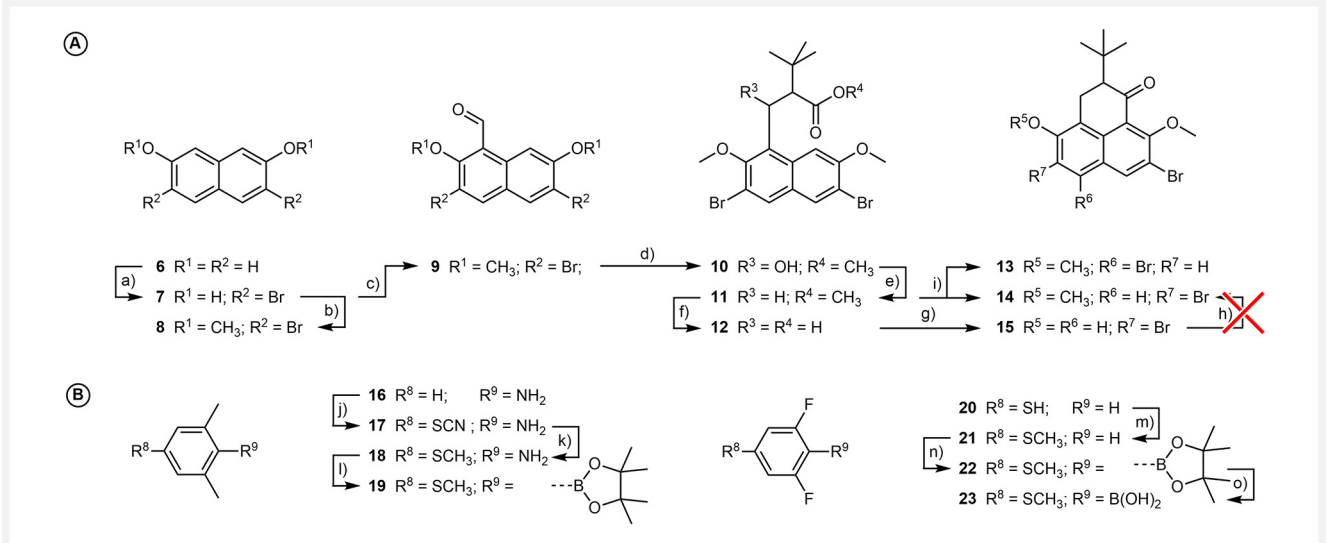

Scheme 2 Synthesis of **A)** the dibromo precursor **14** as a key compound of the modular synthesis, and **B)** the boronic acid derivatives **19** and **23** required for the subsequent Suzuki-type coupling chemistry. Reagents and conditions: a) 1. Br_2, AcOH, reflux, 18 h, 2. Sn, AcOH, reflux, 17 h; b) MeI, K_2CO_3, acetone, r.t. 19 h; c) $TiCl_4$, Cl_2COCH_3, DCM, 0 °C–r.t., 15 h; d) LDA, methyl *tert*-butylacetate, THF, 0 °C, 40 min; e) Et_3Si, TFA, DCM, r.t., 20 h; f) KOH, ethylene glycol, 150 °C, 15 h; g) 1. $(COCl)_2$, 65 °C, 3 h, 2. DCM, $AlCl_3$, −78 °C–r.t. 11 h; h) Table S3 i) TfOH, DCM, r.t., 2.5 h; j) NH_4SCN, trichloroisocyanuric acid, DCM, wet silica, air, r.t., 45 min; k) 1. Na_2S, EtOH, H_2O, 50 °C, 2 h, 2. MeI, EtOH, 3 h, r.t.; l) B_2Pin_2, ^tBuONO, CH_3CN, reflux, 9 h; m) MeI, K_2CO_3, CH_3CN, 16 h, r.t.; n) 1. *n*-BuLi, THF, −78 °C 2 h, 2. *iso*PrBPin, −78 °C–r.t. 16 h.; o) $MeB(OH)_2$, 0.2 M HCl, acetone, r.t., 8 h.

distillation over triflic anhydride[64] reduced the reaction time to 2 h at r.t., but also resulted in the formation of the demethylated derivative **15** as a sideproduct.

With the availability of the key intermediate **14**, our focused moved to the assembly of the boronic acid derivatives as reaction partners for the further decoration of **14** by cross-coupling protocols. Both the 3,5-dimethylthioanisole-4-pinacolborane **19** and the 3,5-difluorothioanisole-4-boronic acid **23** were prepared in three steps (Scheme 2B).

Thiocyanation of 2,6-xylidine following a literature-known procedure yielded **17** in 48%.[65] Conversion of the thiocyano group of **17** to the methyl-sulfide gave **18** in 83% yield following a patented procedure.[66] The amine was converted to the corresponding boronic ester in a Sandmeyer-type reaction following a previously published protocol,[67] yielding the pinacolborane **19** in low 16% isolated yield.

Methylation of 3,5-difluorobenzenethiol **20** with methyl iodide as reported in a patented procedure[68] and subsequent borylation following a published protocol[69] yielded the pinacolborane **22** in an excellent yield of 96% over both steps. Using a previously published trans-esterification procedure, employing methyl boronic acid in a 1 : 1 mixture of aqueous 0.2 M HCl and acetone yielded quantitatively the desired boronic acid **23**.[70] The transformation to the boronic acid became necessary as the boronic ester displayed poor reactivity in the envisaged Suzuki cross-coupling reaction.

With the precursors **14, 19**, and **23** in hands, the Suzuki cross-coupling protocol was developed. Screening of the reaction conditions with **14, 22**, and **23** revealed that the boronic acid derivative **23** and the dibromide **14** using potassium fluoride in combination with $Pd_2(dba)_3$/P(*t*-Bu)$_3$ as a catalytic system provided a clean, fast and high yielding transformation to the desired product **24**, which was isolated in 93% yield (see Table S3, entry 5). Applying similar conditions to **14** and **19** gave the desired compound **25** in 45% isolated yield.

Reducing the carbonyl of **24** and **25** with DIBAL-H in dry THF at 0 °C yielded the desired hydroxyls **29** and **30** in excellent yields of 92% and 95%, respectively.

Removal of the ether protection group was investigated first with compound **30**. Applying a modified reported protocol using LiI in DMPU (HMPA was replaced by DMPU due to its lower toxicity[71]) provided the desired 6-hydroxyphenalenone **2** in 87% isolated yield after acidic work-up. However, employing similar reaction conditions to **29** did not provide the desired 6-hydroxyphenalenone **1**, but the phenaleno[1,2-b]benzofuran derivative **1′** was formed upon intramolecular substitution of a fluorine by the neighbouring hydroxy group, which was isolated in excellent 90% yield (Scheme S1). To avoid this efficient but undesired reaction, a Lewis acid-mediated ether cleavage with BBr_3 was employed, which resulted in the desired compound **1** in 44% yield. Applying these reaction conditions to **30** not only gave lower yields of 36%, but also the degradation of the formed product **2** was observed under these conditions.

The family of 2,5-diaryl 6-hydroxyphenalenones was enlarged by the structures **3**–**5** as model compounds for spectroscopic analysis. These structures do not expose an anchoring group but have electronically neutral (**3**), donating (**4**), or withdrawing (**5**) substituents instead. For their assembly the synthetic protocol developed for **1** and **2** was applied.

Treating the key intermediate **14** with the corresponding, commercially available, arylboronic acids, followed by reduction and de-protection, provided 2,5-diphenyl 6-hydroxyphenalenone **3**, 2,5-di(4′-*tert*-butylphenyl) 6-hydroxyphenalenone **4**, and 2,5-di(4′-fluorophenyl) 6-hydroxyphenalenone **5** in 31%, 31% and 36% over three steps, respectively. Interestingly, the final ether cleavage was only successful with LiI in DMPU at 170 °C, which gave the desired target structures in moderate yields, while treatment with BBr_3 resulted in degradation of all three compounds.

The hydroxyl groups of the 6-hydroxyphenalenone derivatives displayed their acidity by broad peaks in the NMR spectra (Figure S242) and partial deprotonation is observed in the UV-Vis spectra recorded in acetonitrile/water mixtures (Figure S15). By buffering the spectroscopic samples with trifluoroacetic acid, complete protonation was achieved facilitating the interpretation of the spectroscopic data.

Radical Formation and Characterization

The radicals **1R** and **2R** of the 6-hydroxyphenalenone derivatives **1** and **2**, respectively, were obtained in quantitative yields by treating a degassed 5 mM solution in toluene or benzene with freshly precipitated lead dioxide (Scheme 3e).[72] The lead dioxide was subsequently removed by filtration under argon. Attempts to isolate the radical by evaporation of the solvent at the rotary evaporator failed, as the radicals quantitatively degraded to the parent 6-hydroxyphenalenone precursors. Further studies were thus performed with the filtered solution obtained after removal of the lead dioxide.

The radical nature of **1R** and **2R** was verified by X-band electron paramagnetic resonance (EPR) and UV-Vis spectroscopy. The UV-Vis spectrum of **1R** shows a very broad but not very intense absorption band at λ_{max} = 753 nm, a broad feature at λ_{max} = 498 nm and two sharp features at 409 and 390 nm (Figure 2A). However, the UV-Vis spectrum of **2R** shows a very broad band at λ_{max} = 786 nm, a slanted feature at λ_{max} = 581 nm and two sharp features at 415 and 395 nm (Figure 2B). The two recorded UV-Vis spectra differ mainly in intensity of the observed features, while their shape is rather similar, both show a broad feature in the red to near-IR part of the absorption spectra and two sharp fea-

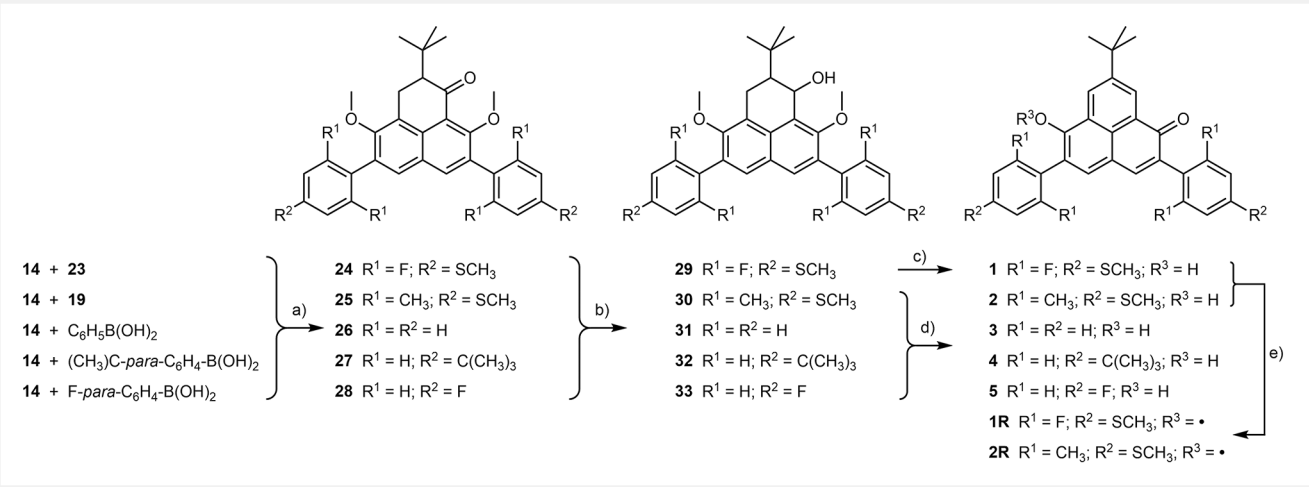

Scheme 3 Assembly of the target structures. Reactions and conditions: a) $Pd_2(dba)_3$, $P(^tBu)_3$, KF, THF, H_2O, 70 °C, 3 h, b) DIBAL-H, THF, 0 °C, 2 h, c) 1. LiI, DMPU, 170 °C, 18 h, 2. 6 M HCl, d) 1. BBr_3, DCM, −78 °C–r.t., 16 h, 2. 6 M HCl, 30 min, e) PbO_2, dry toluene, 1 h, protected from light, moisture and air.

tures between 390 and 420 nm. Additionally, the spectrum of **1R** is blueshifted with respect to the spectrum of **2R**. Toluene/benzene solution of both radicals **1R** and **2R** did not show any fluorescence properties, indicating the complete consumption of the fluorescent precursors **1** and **2**. The recorded UV-Vis absorption spectra of **1R** and **2R** resemble reported electronic absorption spectra of oxophenalenoxyl radicals.[51]

The radical nature of **1R** and **2R** was definitively confirmed by EPR spectroscopy. EPR directly probes the unpaired electron spin and its interaction with neighbouring nuclei with a nuclear spin through hyperfine coupling. EPR signals of organic radicals are isotropic and reported by the *g*-value centering the EPR signal. The obtained EPR spectra of the oxophenalenoxyl radicals **1R** and **2R** in toluene are shown in Figure 2C and 2D. The determined *g*-values are 2.0032 and 2.0031, respectively, comparable to the reported values of oxophenalenoxyl derivatives in the literature.[51,52,73] The *g*-values of **1R** and **2R** have a positive deviation from the g_e-value = 2.0000 of a free electron, which is an indication that the SOMO level of the organic radical is located closer to the HOMO than the LUMO level.[74] For both EPR spectra, no clear hyperfine splitting was observed, in spite of the presence of various EPR active nuclei (H^1 and in case of **1R** also F^{19}). Nevertheless, barely visible shoulders at *g*-values of ~2.0026 and ~2.0040 for **1R** (Figure 2C) and **2R** (Figure 2D) are observed, respectively, indicative of some degree of magnetic coupling between the radicals and nuclear spin(s) in both cases. The lack of hyperfine coupling is likely due to the X-band nature of the EPR experiments, and access to higher frequencies such as Q-band EPR might have resolved this matter. Although no resolved hyperfine splitting was observed, both X-band EPR spectra verify the radical nature of **1R** and **2R**. Furthermore, treatment of both radicals in benzene/toluene with hydrazine monohydrate in a UV-Vis experiment yielded quantitatively the corresponding 6-hydroxyphenalenone derivatives **1** and **2** (Figure S249).

Attempts to crystallize the radicals **1R** and **2R** were performed by solvent layering. And indeed, slow diffusion of *n*-hexane into a solution of **1R** dissolved in toluene at 0 °C provided red cubic crystals suitable for X-ray analysis. However, the obtained crystal structure (Figure 3) was the one of the 6-hydroxyphenalenone **1**, pointing at the limited stability of the radical structure **1R**. To investigate the radicals' stability, the temporal development of their UV-Vis spectra was recorded in toluene at room temperature (Figures S18 and S45). Half-life periods of 33 h for **1R** and 25 h for **2R** were determined in the dark without additional measures to protect the solutions from moisture and/or oxygen.

All intermediates and target structures were fully characterized by ^{1}H- and ^{13}C-NMR spectroscopy and high-resolution mass spectrometry. The target structures were additionally analysed by UV-Vis spectroscopy and voltammetry. The complete analytical data as well as the corresponding spectra are provided in the Supplementary Information.

Crystal Structure of 6-Hydroxyphenalenone 1

As already mentioned above, the crystal structure of **1** was obtained upon unsuccessful attempts to crystallize the radical **1R. 1** and **1R** can easily be distinguished by bond lengths in the solid-state structure, as for **1R** similar bond length for both C – O bonds are expected, while the 6-hydroxyphenalenone **1** exhibits different bond lengths for the carbonyl C=O and the hydroxyl C – O bond. The crystal structure displays bond lengths of 1.25 and 1.34 Å corroborating the 6-hy-

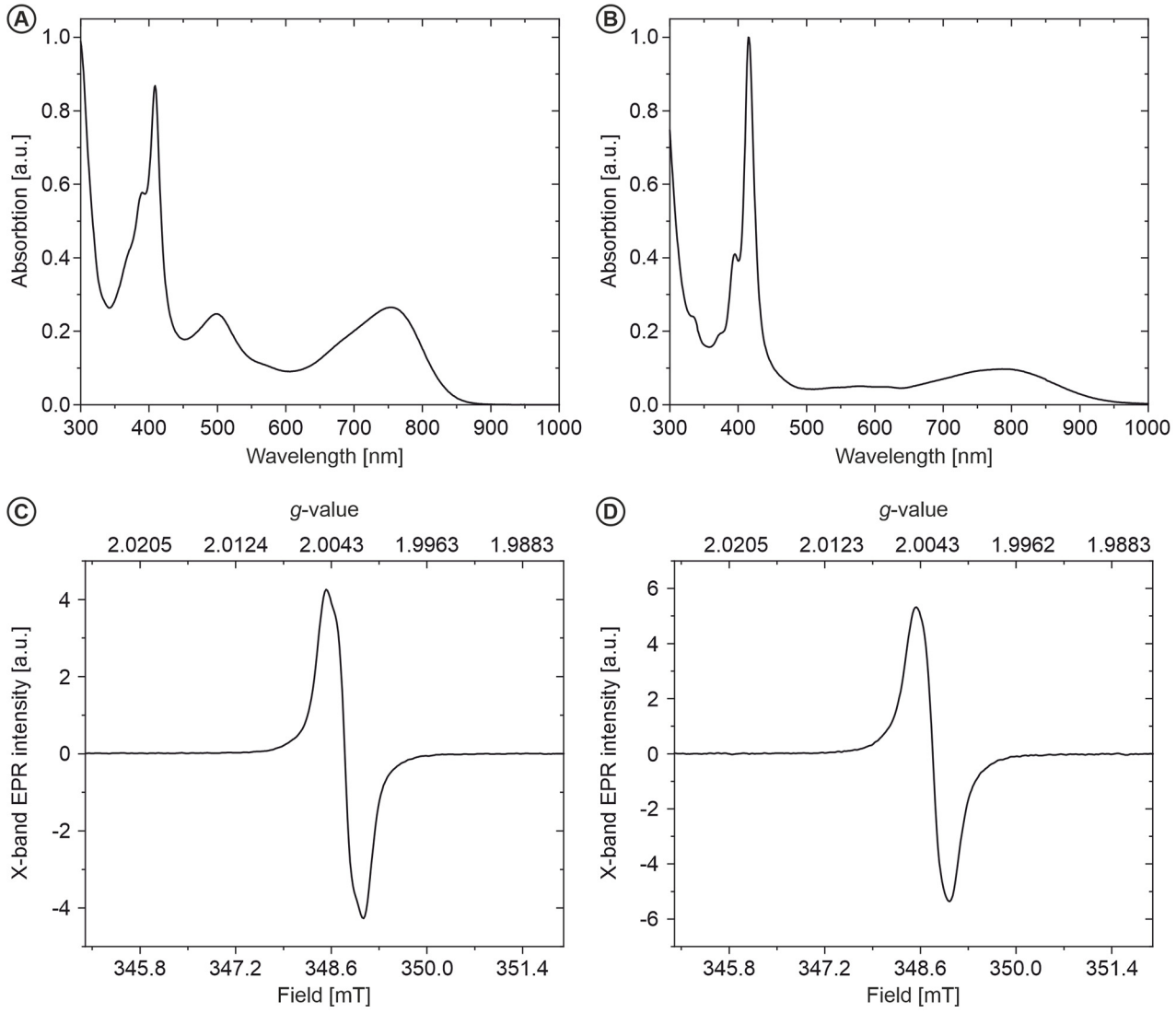

Figure 2 UV-Vis absorption and EPR measurements: **A)** and **B)** show the UV-Vis absorption spectra recorded after exposing 6-hydroxyphenalenones **1** and **2** to freshly precipitated PbO_2 in dry deaerated toluene protected from light. **C)** and **D)** show the EPR spectra recorded form their respective radicals **1R** and **2R** in toluene at room temperature.

droxyphenalenone core structure. The solid-state structure further provided insight into the degree of aromatization within the structure subunits. The bond lengths of the two 3,5-difluorothioanisole substituents (rings *D* and *E* in Figure 3) are all quite comparable: 1.37 Å and 1.39 Å, pointing at an aromatic system with equilibrated bond lengths. A much wider length distribution is, however, recorded for the 6-hydroxyphenalenone core (rings *A*, *B*, and *C* in Figure 3), with values ranging from 1.36 to 1.48 Å.

While for ring *A*, the bond lengths remain between 1.38 and 1.42 Å and thus it can still be considered as an aromatic system; the rings *B* and *C* of the naphthalene substructure show an even wider C–C bond length distribution ranging from 1.36 to 1.48 Å. In addition, the bond lengths are alternating along a path through the naphthalene between both oxygen atoms (orange coloured in Figure 3A). All other bonds in the naphthalene substructures remain between 1.414 and 1.475 Å. Based on these observations, it seems that the electronic pathway through the 6-hydroxyphenalenone core is better described as a discrete conjugated system consisting of alternating single and double bonds than as a delocalized π-system. The carbon atoms 2 and 5 of the 6-hydroxyphenalenone core are part of the electronic pathway, such that the current passing through the substituents

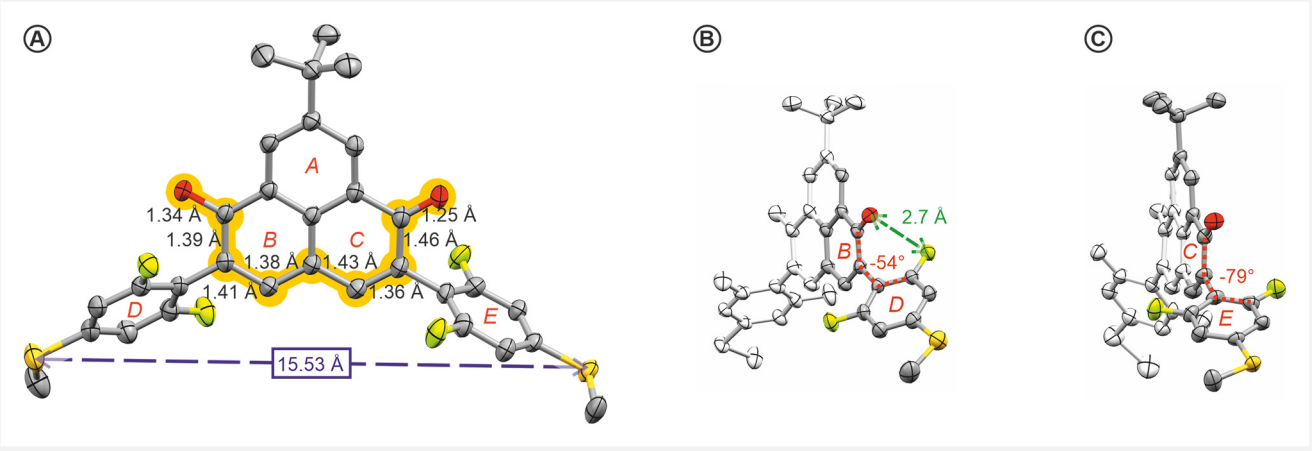

Figure 3 Crystal structure of **1** recorded at 150 K. Hydrogen atoms are omitted for clarity: **A)** frontal view of **1**; the sequence of alternating bond lengths through the bottom of the naphthalene sub-structure is highlighted by a dark yellow background. The dotted dark blue dashed arrow displays the sulphur-to-sulphur distance of 15.53 Å. **B)** Side view facing the hydroxyl substituent. The green dashed arrow indicates the oxygen fluorine distance of 2.7 Å. The red-dotted lines indicate the torsion angle of −54° between ring *B* and ring *D*. **C)** Side view facing the carbonyl substituent. The red-dotted line indicates the torsion angle of −79° between ring *C* and ring *E*.

mounted at these positions most likely follows that pathway too. The 2,6-difluorothioanisole substituents at the positions 2 and 5 display different torsion angles with respect to the 6-hydroxyphenalenone core.

The torsion angle between thioanisole ring *E* and the ring *C* (Figure 3C) is by 25° larger than the torsion angle between the thioanisole *D* and the ring *B* (Figure 3B). This difference in torsion angle can be rationalized by the hydroxyl forming hydrogen bonds with one of the fluorine atoms of the adjacent thioanisole *D*. And indeed, the fluorine–oxygen bond distance of 2.7 Å (Figure 3B) supports this hypothesis. Considering the bond length of an oxygen–hydrogen bond of ~0.8 Å, a hydrogen-to-fluorine distance of ~1.8 Å can be estimated, matching well with reported H···F hydrogen bonds.[75]

UV-Vis Analysis

The UV-Vis spectra of the 6-hydroxyphenalenone derivatives (**1**–**5**) were recorded in acetonitrile with 1% TFA as an acidic buffer to observe the protonated species and in MeOH with additional 10% of an aqueous 2 M KOH solution to characterise the deprotonated compounds. Derivative **2** displays a low enough acidity that it was not necessary to add TFA to obtain a UV-Vis spectra of the protonated form. However, the other derivatives did show slight deprotonation and therefore required addition of TFA. TFA was chosen because it hardly affected the absorption spectrum of **2**. With the exception of a small redshift (3 nm) of the λ_{max} absorption band at 444 nm (Table 1, entry 2 (red)), all other absorption signals of **2** remained unaffected. The UV-Vis spectra for all protonated and all deprotonated 6-hydroxyphenalenone derivatives have very comparable shapes (Table 1, top). Looking at the spectra recorded in acetonitrile (Table 1, top, **A** and **B**), it is clearly visible that the two thioanisole derivatives **1** and **2** show a blueshift in both the absorption and emission properties compared to the phenyl derivatives **3, 4** and **5**. In addition, a redshift in absorption and emission for increasing electron density of the thioanisole substituents can be observed. The redshift for increasing electron density is also visible for the three phenyl derivatives **3, 4** and **5**, although the electron-donating *tert*-butyl group of **4** seems to have a stronger electronic influence compared to the electron-withdrawing fluorine substituent of **5**, as **5** and **3** show almost identical absorption and emission spectra.

Interestingly, the fluorescence quantum yield (QY) increases with increasing electron deficiency as can be seen in Table 1. The QY of the 3,5-difluorothioanisole derivative **1** shows an increase of 14.7% compared to that of the dimethyl derivative **2**. The same electronic effect on the QY is observed for the phenyl derivatives **3**–**5**, where **4** shows the lowest while **5** shows the highest QY of the three phenyl derivatives.

The optical properties recorded in basic media behave similar to the native 6-hydroxyphenalenone derivatives, an increase in QY upon reduction of the electron density as well as a clear redshift for increasing electron density was observed (Table 1). A strong redshift in both the absorption and emission bands upon deprotonation accompanied by a large increase in QY is observable for all 6-hydroxyphenalenone derivatives. For example, the absorption λ_{max} of **2** shifts from 447 to 579 nm and the QY increases from 7.2 ± 0.9% to 46 ± 0.5% upon deprotonation. This redshift as well as the large increase in QY indicates the increased aromaticity in the central phenalenon structure upon depro-

Table 1 UV-Vis absorption and emission properties of the 6-hydroxyphenalenone derivatives **1 – 5**

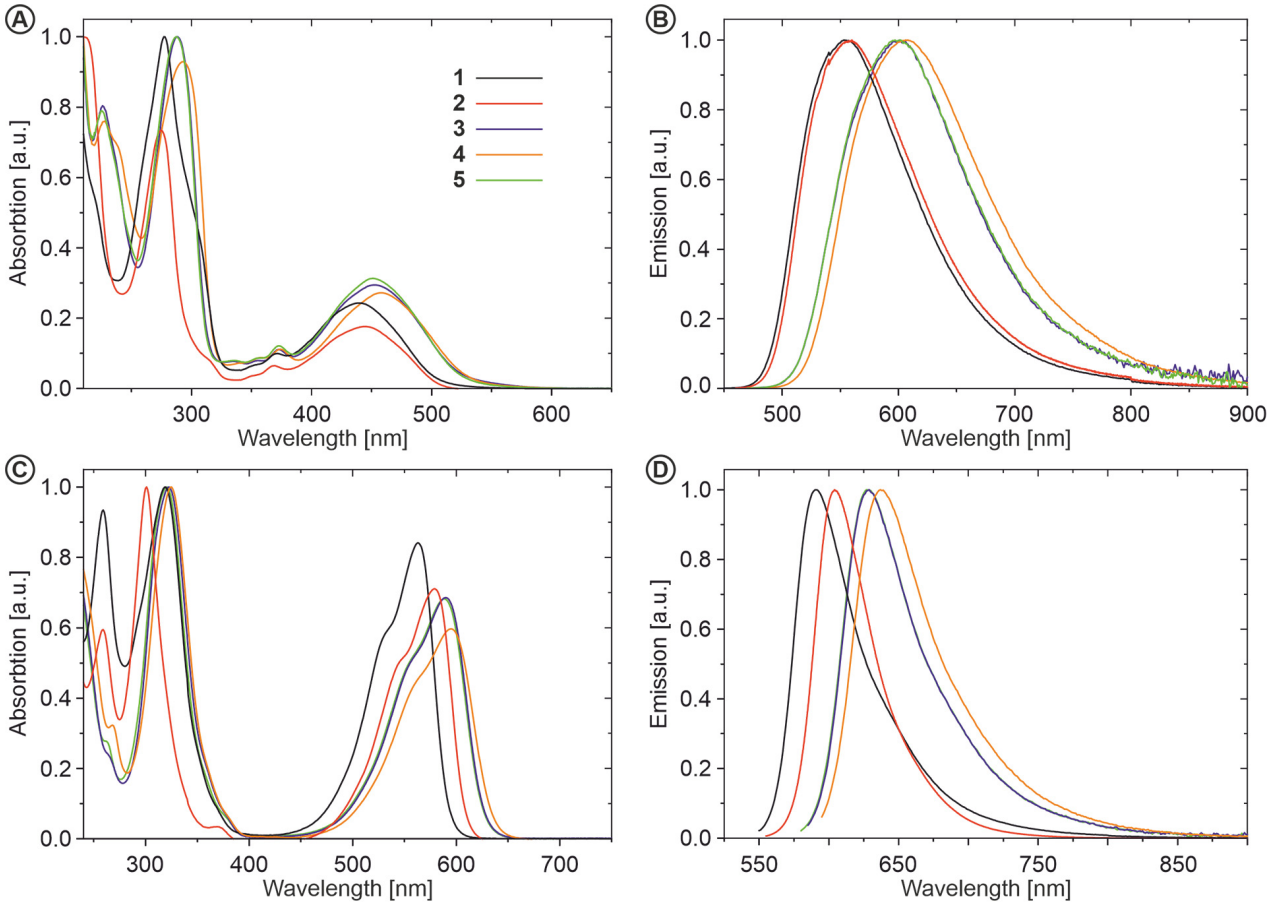

6-Hydroxyphenalenone derivative	ACN (1 % TFA) absorption [nm]	ACN (1 % TFA) emission [nm]	Int. quantum efficiency [%] ACN (1 % TFA)	MeOH (10 % 2 M KOH) absorption [nm]	MeOH (10 % 2 M KOH) emission [nm]	Int. quantum efficiency [%] MeOH (10 % 2 M KOH)
1 (black)	440, 371, 277	553	21.9 ± 1.8	563, 319	591	52.4 ± 1.0
2 (red)	447/444[a], 369/369[a], 275/275[a]	559.8	7.2 ± 0.9	579, 301	604	46.1 ± 0.5
3 (blue)	452, 372.5, 288	601	14.6 ± 0.4	590, 322.5	629	24.0 ± 0.3
4 (orange)	458, 375, 293	606	10.9 ± 0.5	594, 324	637	21.6 ± 0.4
5 (green)	450, 372.5, 287.5	602	15.0 ± 0.2	588.5, 320.5	627	33.1 ± 1.1

The 6-hydroxyphenalenone derivatives are colour-coded with **1** (black), **2** (red), **3** (blue), **4** (orange), and **5** (green). **A)** Absorption spectra and **B)** emission spectra recorded in acetonitrile with 1 % TFA to ensure complete protonation of the 6-hydroxyphenalenone, **C)** absorption spectra and **D)** emission spectra recorded in MeOH with 10 % 2 M KOH to ensure complete deprotonation of the 6-hydroxyphenalenone · [a]No TFA additive.

tonation. Another general observation is that the thioanisole derivatives (**1** and **2**) show blueshifted absorption features accompanied by an increased QY compared to the phenyl derivatives.

Electrochemical Analyses

The redox properties of the 6-hydroxyphenalenone derivatives **1**–**5** were of particular interest considering their potential as electrochemically triggered switches, and were investigated by CV. In the case of irreversible oxidations or reductions in the recorded CVs, the analyses were comple-

mented by square wave voltammetry (SWV). CVs of 6-hydroxyphenalenone derivatives **1**–**5** were recorded in dry deaerated acetonitrile with 0.1 M NBu_4PF_6 as the supporting electrolyte. Decamethylferrocene ($Me_{10}Fc$) was used as an internal standard in the redox experiments, due to its oxidation signal, which is with $E_{1/2}(Me_{10}Fc^+/Me_{10}Fc)$ = −0.096 V vs. saturated calomel electrode (SCE)[76] outside the redox signals of 6-hydroxyphenalenone derivatives.

The CV recorded for **1** showed two reversible redox couples at $E_{1/2}$ = 0.42 V and $E_{1/2}$ = −1.81 V vs. SCE (Figure 4A). The reversibility of the redox couples was corroborated by the linear relationship between the peak current and the scan rate in the Randles–Ševčík plot (Figure 4C). The remaining 2,5-diaryl 6-hydroxyphenalenones **2**–**5** displayed mainly irreversible redox signals. The exception was **5** with electron-deficient aryl substituents, which showed reversible redox couples at $E_{1/2}$ = −1.90 V and $E_{1/2}$ = −2.17 V against SCE (Figure S88). Again, the Randles–Ševčík plot corroborated the reversibility of these redox events (Figure S88E). As an example of a compound with irreversible redox events, the CV and SWV of **2** are displayed in Figure 4B. A multitude of peaks were observed, from which some were attributed to

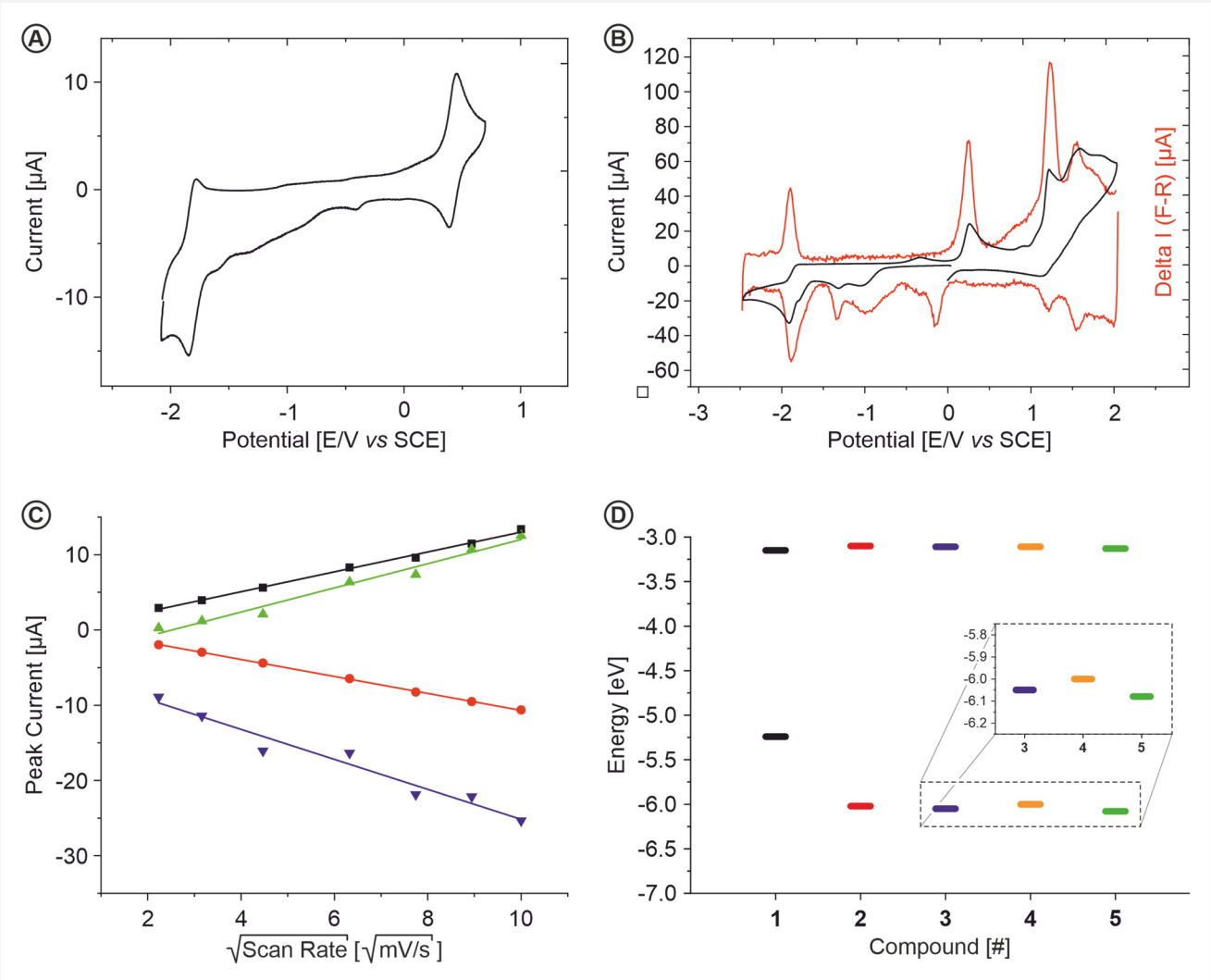

Figure 4 Electrochemical analysis of the 6-hydroxyphenalenone derivatives recorded in acetonitrile with 0.1 M NBu_4PF_6 as a supporting electrolyte at r. t. All spectra were calibrated against the $Me_{10}Fc^+/Me_{10}Fc$ couple and are reported against SCE: **A)** the CV of **1** (1.4 mM). The spectrum shows two clear redox couples one at $E_{1/2}$ = 0.42 V and one at $E_{1/2}$ = −1.81 V. **B)** The CV (in black) and the SWV (in red) of **2** (2.4 mM). The voltammogram shows an irreversible oxidation at E_{onset} = 1.13 V and reduction at E_{offset} = −1.8 V. **C)** Randles–Ševčík plot of the redox couples shown in **A)** determined form the isolated couples. The lines in black and red correspond to the couple at $E_{1/2}$ = 0.42 V, while the green and blue lines correspond to the couple at $E_{1/2}$ = −1.81 V. All lines show a prefect linear fit confirming full reversibility of both redox couples over all recorded scan rates. **D)** The HOMO and LUMO level energies of the 6-hydroxyphenalenone derivatives **1**, **2**, **3**, **4** and **5** are shown in black, red, orange, green and blue, respectively. The inset shows a zoomed-in view of the HOMO levels of **3**, **4** and **5**.

degradation products. During the CV and SWV experiments, the formation of an orange layer at the electrode surface was observed, pointing at insoluble degradation products.

By scanning exclusively negative or positive scan regions, the two pronounced peaks at −0.16 V and 0.20 V vs. SCE visible in the SWV as well as the CV spectra of **2** were identified as emerging from degradation products, which arise from the irreversible oxidation and reduction at E_{onset} = 1.13 V and E_{offset} = −1.8 V vs. SCE, respectively.

The HOMO and LUMO levels were estimated using the empirical relationship reported by Janssen et al.[77] based on the oxidation and reduction potentials of **1**–**5.** The determined energy levels of the frontier orbitals are displayed in Figure 4D. While the LUMO levels of the investigated compounds seem to be overall unaffected by the different aryl substituents, the HOMO levels display more variation. Considering only the small series **3**–**5** without a methyl-sulfide anchoring group, the variation can be rationalized by an inductive effect of the aryl's *para*-substituent. The HOMO level of **4** with 4-*tert*-butyl phenyl groups is slightly higher than the one of **3** with phenyl groups, and that of the latter is slightly higher than the one of **5**, with 4-fluorophenyl groups. A HOMO level of comparable energy was also recorded for **2**, with a methyl-sulfide group at the *para*-position and two methyl groups at both *ortho*-positions. The pronounced increase of the HOMO energy of **1** by 0.78 eV compared to **2** was surprising. The structural differences between **1** and **2** are only the four *ortho*-substituents of the thioanisoles. While the methyl *ortho*-substituents of **2** are inductively electron-donating, the fluorine atoms of **1** are inductively electron-withdrawing. However, due to the fluorine lone pairs they have a donating mesomeric effect, which might excel the inductive effect. The intramolecular H···F bond between the hydroxyl group and a fluorine atom already observed in the solid-state structure might impact the redox properties, as has been reported for the oxidation potential of other redox systems.[78,79] Finally, also steric effects like the increase of the π-system due to coplanar arrangements of the aryl substituents as already hypothesized in the discussion of the UV spectra might contribute to the considerably increased HOMO energy of **1** relative to **2**.

However, the shape of the UV-Vis spectra of the series **1**–**5** was mainly dictated by the 6-hydroxyphenalenone core.

The different aryl substituents did not affect the shape of the spectra, but only caused a red- or blueshift depending on the electron density of the substituent. Whereas the redox properties seem to strongly reflect the nature of the aryl substituents.

Spectroelectrochemical Analysis

To identify and characterize the species formed in the electrochemical experiment, UV-Vis spectra of **1** were recorded in situ while an electrochemical experiment was performed. A solution of **1** in acetonitrile with 0.1 M NBu_4PF_6 as the supporting electrolyte was exposed to oxidising and reducing potentials. The obtained differential UV-Vis spectra and the obtained isosbestic points are shown in Figure S17. The applied potentials were chosen to be slightly more negative or positive than the redox couples determined by CV (Figure 4A). In the spectroelectrochemical investigation, decamethylferrocene was not added as an internal standard, to avoid an additional species in the UV-Vis spectra. Instead, a silver wire was used as a pseudo-reference.

The reducing potential was set to −1.8 V, which is just below the redox couple with $E_{1/2}$ at −1.72 V vs. $Me_{10}Fc^+/Me_{10}Fc$ and above −1.9 V, which is the point at which the solvent starts to degrade. Applying a potential of −1.8 V led to the formation of several new bands (red in Figure 5A), while the bands of the original spectrum vanished (black in Figure 5A). The dynamic changes in the spectra of **1** upon applying −1.8 V are displayed in Figure 5A. The new λ_{max} at 562 nm with a shoulder at 533 nm fits perfectly to λ_{max} at 563 nm of **1** in MeOH and 10% 2 M KOH. Interestingly, the broad absorption band at 319 nm seems to split into two distinct peaks with maxima at 360 and 328 nm. Also the high energy absorption band at 260 nm was detected in the UV-Vis spectrum of **1** recorded in MeOH and 10% 2 M KOH. In conclusion, the species formed from **1** upon applying a reduction potential of −1.8 V corresponds to the anionic form of **1** (Figure 1C).

Upon applying an oxidizing potential of 1 V just above the offset potential of 0.78 V of the redox couple at $E_{1/2}$ = 0.52 V vs. $Me_{10}Fc^+/Me_{10}Fc$ of **1**, a very broad absorption band with λ_{max} at 765 nm arises from the baseline. Thereafter, two very sharp features are observed at 409 and 387 nm (Figure 5B). The evolution of the spectra of **1** upon applying 1 V is displayed in Figure 5B. The final spectrum (red in Figure 5B) resembles the one obtained for **1R**, upon treating **1** with PbO_2 in dry deaerated dry toluene (Figure 2B). The spectrum recorded in toluene is slightly blueshifted compared to the one obtained after electrochemical oxidation in acetonitrile. Nevertheless, the good fit of the data corroborates that the electrochemically formed species is the neutral radical **1R** (Figure 1C). Interestingly, a further increase of the potential to 1.3 V resulted in the degradation of **1R**, indicated by the disappearance of all major absorption peaks above 400 nm.

Single-Molecule Transport Studies

As already elucidated in the Introduction, the motivation to develop the 2,5-diaryl 6-hydroxyphenalenones was the investigation of externally triggered switching events in single-molecule transport studies. While the electrochemically controlled single-molecule transport experiment has not been performed yet, the samples **1** and **2** exposing methyl-

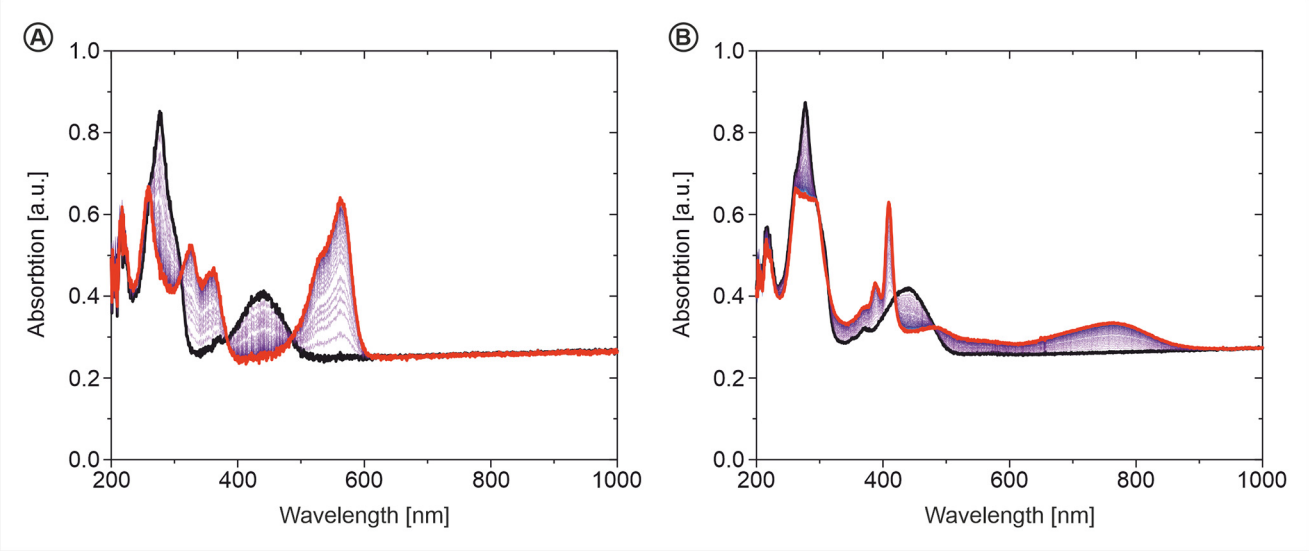

Figure 5 Spectroelectrochemical measurement of **1** in dry deaerated acetonitrile with 0.1 M NBu_4PF_6 as the supporting electrolyte. **A)** The UV-Vis spectra recorded at an applied potential of −1.8 V. **B)** The UV-Vis spectra recorded at an applied potential of 1 V. In black the original spectra whereas in red the newly formed species are indicated. The concentration was chosen such that an absorbance of 0.2 (a. u.) at λ = 440 nm was reached.

sulfide anchor groups should be suited for preliminary transport studies, demonstrating the suitability of the model compounds for molecular junctions. Our focus was set on the structure **1**, which displayed well-addressable redox states in the electrochemical as well as the spectroelectrochemical experiments.

The ability of compound **1** to form single-molecule junctions was thus investigated in a MCBJ experiment. In this type of break junction experiment, a lithographically defined gold nanowire is stretched until it ruptures forming two nanoscale-sized electrodes, while monitoring the current flowing through the system. The electrodes are then further displaced till the monitored current reaches the noise level.

Thereafter, the electrodes are pushed back together to reform the nanowire. The procedure is repeated thousands of times providing large data sets allowing their statistical treatment. If the formed junction is empty, i.e. there is no molecule bridging it, the current decays exponentially with the displacement between the electrodes. If there are molecules bridging the electrodes, the current will be roughly constant for a range of displacement, defining a "molecular plateau." For the measurements, 5 µL of either 1 or 0.1 mM MeOH solution of **1** was drop-casted onto a MCBJ setup. To ensure reproducibility, the measurement was repeated three times with a 1 mM solution and two times with a 0.1 mM solution. If the traces are collected in two-dimensional (2D) conductance-displacement histograms (left panels of Figure 6A – C), the molecular plateau will form a high-counts area that stays constant for a range of displacements proportional to the length of the molecule. On the other hand, empty traces will show only a high-counts area having a steep slope. Considering one-dimensional (1D) conductance histograms (right panels of Figure 6A – C), molecular traces present a characteristic peak, which follows a log-normal shape. The centre of such distribution is the "most-probable conductance" of the molecule. However, empty traces will show a slow increase of the counts with decreasing conductance.[80]

To represent all the measurements in combined histograms, we collected the traces of each measurement and treated it as a single dataset. The collected breaking traces were then used to build the 2D conductance displacement histograms and 1D conductance histograms of Figure 6A. A previously established clustering algorithm[81] was used to isolate the traces containing molecular features (Figure 6B), showing the characteristic peak in the 1D conductance histogram, from the empty ones (Figure 6C). Fitting these histograms of **1**, a conductance plateau at $2.6 \times 10^{-6}\, G_0$ with a length of 1 nm was obtained.

Adding the snapback distance of 0.5 nm to the obtained plateau length yields an absolute displacement of the two electrodes of ~1.5 nm, which is in good agreement with the sulphur-to-sulphur distance of 15.53 Å extracted from the solid-state structure of **1** (Figure 3A).[82,83] The relatively low conductance of **1** was expected for two reasons. First, as already discussed with the solid-state structure, the naphthalene substructure of **1** displayed limited aromaticity and thus also restricted transport features were anticipated. Second, methyl-sulfide anchor groups are chemically robust and are known to yield sharp conductance features, but their

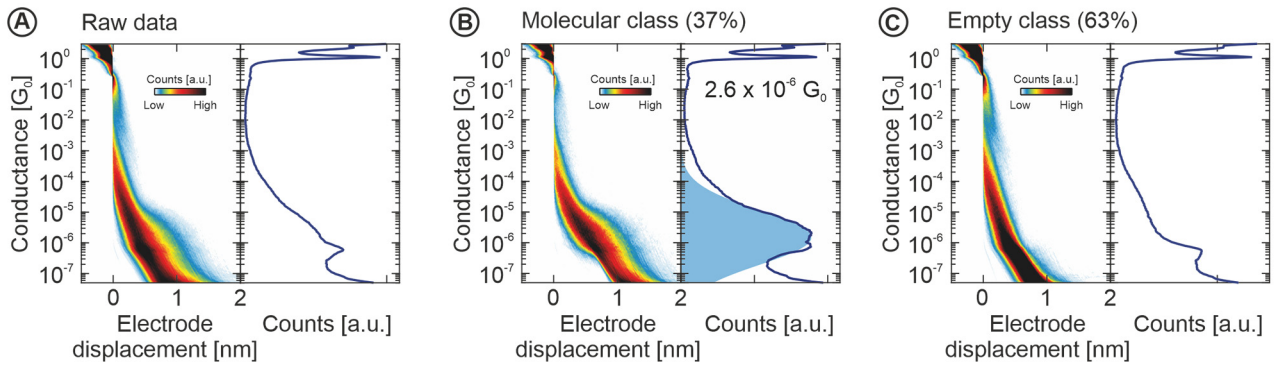

Figure 6 Electronic conductivity measurement of **1** with a MCBJ setup. **A)** The merged raw data from all five performed measurements with a total of 21 927 consecutive breaking traces. **B)** Conduction traces with a molecular conductance contribution identified by an unsupervised clustering algorithm. The clustering method identified in approximately 37 % of all traces a molecular conductance contribution. **C)** Breaking traces in which the clustering algorithm did not identify a molecular conductance contribution. The small peak at around $10^{-6}\,G_0$ is an artefact originating from the electronics employed during the measurement. It is mostly present in the rapidly decaying empty traces, and thus it is not a molecular feature.

transparency for electric currents is known to be considerably smaller than, e.g., thiol anchor groups.[84,85]

More information on the methodology and an overview of all five measurements are provided in the Supplementary Information (MCBJ Measurements of **1** and their Analysis).

Conclusions

A universal synthetic strategy towards 6-hydroxyphenalenone derivatives using the versatile key intermediate **14** is reported. Using this strategy, five derivatives with different aryl substituents were synthesized and their properties were investigated by optical spectroscopy and electrochemical experiments. Two of the model compounds (**1** and **2**) expose methyl-sulfide anchoring groups making them suitable candidates for the formation of molecular junctions. From both structures the oxophenalenoxyl radicals **1R** and **2R** were obtained by wet chemical treatment with PbO_2. Spectroelectrochemical studies demonstrate that the radical **1R** can also be obtained electrochemically, by oxidizing a sample of **1**. The electrochemical reversibility of the redox events of **1** demonstrates its suitability for electrochemically addressed single-molecule junctions. And indeed, preliminary MCBJ experiments show the efficiency of **1** in the formation of molecular junctions. In particular, a conductance plateau at $2.6 \times 10^{-6}\,G_0$ with a plateau length of 1 nm is observed.

Currently, we are exploring the here-presented model compounds **1** and **2** as molecular switches in MCBJ experiments, triggered either by wet chemical reagents or by electrochemical means.

Experimental Section

Dry diisopropylamine was obtained by distillation from sodium hydride under argon. Dry THF, dioxane, toluene and benzene were obtained by distillation from sodium and benzophenone under argon. All other chemicals and anhydrous solvents were used as purchased without further purification, unless stated otherwise. Deuterated solvents were obtained from Cambridge Isotope Laboratories, Inc. (Andover, MA, USA). All other commercially available starting materials and solvents were purchased from Honeywell, Sigma-Aldrich, Acros or Fluorochem. NMR experiments were performed on a 400 or 500 MHz Bruker Avance III spectrometer equipped with a QNP or BBFO probe head, respectively. All 600 MHz spectra were recorded on either a Bruker Avance III NMR spectrometer operating at 600.13 MHz proton frequency equipped with a direct observe 5 mm BBFO smart probe or an indirect 5 mm BBI probe or a Bruker Avance III HD NMR spectrometer operating at 600.13 MHz proton frequency equipped with a cryogenic 5 mm four-channel QCI probe (H/C/N/F). All spectra were recorded at 298 K. The chemical shifts (δ) are reported in parts per million (ppm) relative to tetramethylsilane or referenced to residual solvent peaks and the *J* values are given in Hz (± 0.1 Hz). EPR spectra (X-band) were recorded on a Bruker ELEXSYS-II E500 CW-EPR spectrometer. Samples for EPR measurements were prepared in capillary tubes and measured at r. t. For HRMS, a HR-ESI-ToF-MS measurement on a maXisTM 4 G instrument from Bruker was performed. Gas chromatography-mass spectrometry (GC-MS) results were recorded using a Shimadzu GC-MS-2020-SE instrument equipped with a Zebron 5 MS Inferno column, with a temperature range of up to 350 °C. Column chromatography was performed on SiliaFlash®P60 from SILICYCLE with a par-

ticle size of 40 – 63 µm (230 – 400 mesh). TLC was performed on Silica gel 60 F254 glass plates with a thickness of 0.25 mm from Merck using fluorescence quenching under UV light at 254 nm for the localization of sample spots. Automated recycling GPC was performed on a Shimadzu Prominence System equipped with two SDV preparative columns in series from Polymer Standards Service (PSS) (20 × 600 mm each, exclusion limit: 30 000 g/mol). UV-Vis absorption spectra were recorded at 20 °C on a Jasco V-770 spectrophotometer. UV-Vis emission spectra were recorded at 20 °C on a JASCO Spectrofluorometer FP-8600. CV was performed in an MBraun Glovebox under argon. As a working electrode, a glassy carbon disk electrode was used while as a counter and (pseudo-) reference electrode a silver wire was used. The voltage was applied and controlled with a VersaSTAT 3 – 200 potentiostat from Princeton Applied Research. SWV experiments were recorded at a frequency of 100 Hz with a step height of 10 mV and a pulse height of 25 mV was chosen. All presented data were taken from the first scan to exclude effects of repetitive oxidation and reduction on the voltammogram. If the first scan did start with a current dip, the data were taken after the dip. Spectroelectrochemical measurements were performed in an argon-filled glovebox from MBraun using a fibre-based UV-Vis absorption setup. A platinum grid electrode was used as a working electrode in a quartz cuvette. A silver wire, which was separated from the analyte solution by a frit, served as a pseudo-reference electrode and a platinum wire was employed as a counter electrode. To apply and control the potential, a VersaSTAT 4 potentiostat from Princeton Applied Research was employed. As a light source, a DH-mini UV-Vis-NIR Deuterium–Halogen source from Ocean Insight was used and an Ocean HDX-XR spectrometer served as the detector. IR spectra were recorded with a Shimadzu IRTracer-100.

8-(*Tert*-butyl)-2,5-bis(2,6-difluoro-4-(methylthio)phenyl)-6-hydroxy-1*H*-phenalen-1-one 1: A round bottom flask was charged with compound **29** (20.0 mg, 32.4 µmol, 1 equiv) dissolved in dry DCM (5 mL) and purged with argon for 15 min. The mixture was then cooled to 0 °C. Thereafter, BBr_3 (0.01 mL, 99%, 100 µmol, 3.1 equiv) was added dropwise and the mixture was left to warm up to r.t. over 16 h. The reaction was then quenched by careful addition of aq. 6 M HCl and stirred for another 30 min and then poured into ice water and extracted with DCM (two times). The combined organic was washed with brine (two times), dried over anhydrous Na_2SO_4 and concentrated under reduced pressure. The crude was further purified by column chromatography on silica gel (chloroform : pentane 2: 1 0.1% TFA) and reverse phase column chromatography on C^{18} functionalised silica gel (CH_3CN : H_2O 10 : 1 + 0.1% formic acid) yielding **1** (10.0 mg, 18.0 µmol, 54.3%).

^{1}H NMR (600 MHz, $CDCl_3$) δ: 9.00 (s, 2 H), 7.92 (s, 2 H), 6.93 (m, 4 H), 2.53 (s, 6 H), 1.53 (s, 9 H).

^{1}H{^{19}F} NMR (600 MHz, $CDCl_3$) δ: 9.00 (s, 2 H), 7.92 (s, 2 H), 6.93 (s, 2 H), 2.53 (s, 4 H), 1.53 (s, 6 H).

^{19}F NMR (565 MHz, $CDCl_3$) δ: −75.75 (TFA), −110.64.

^{13}C NMR (151 MHz, $CDCl_3$) δ: 170.83, 161.61 (d, J = 8.0 Hz), 161.05 (q, J = 44.0, 43.3 Hz(TFA)), 159.95 (d, J = 8.0 Hz), 151.70, 144.34 (t, J = 10.1 Hz), 143.35, 131.71, 126.24, 125.85, 120.23, 118.54, 114.42 (q, J = 285.0 Hz(TFA)), 109.19 (d, J = 5.3 Hz), 109.04 (d, J = 5.0 Hz), 107.80 (t, J = 20.6 Hz), 35.87, 31.34, 15.16.

^{13}C NMR (151 MHz, $CDCl_3$) dept δ: 143.13, 131.51, 109.21 – 108.75 (m), 31.19, 15.02.

HRMS (ESI) *m/z*:

Calcd. for $[C_{31}H_{24}F_4O_2S_2 + H]^+$ 569.1221 $[M + H]^+$; 569.1227
$[C_{31}H_{24}F_4O_2S_2 + Na]^+$ 591.1044 $[M + Na]^+$; 591.1046
$[C_{31}H_{23}F_4O_2S_2 + 2 \times Na\text{-}H]^+$ 613.0855 $[M + 2 \times Na\text{-}H]^+$; 613.0865.

2-(*Tert*-butyl)-5-(2,6-difluoro-4-(methylthio)phenyl)-8-fluoro-10-(methylthio)-4*H*-phenaleno[1,2-b]benzofuran-4-one 1′: A round bottom flask was charged with LiI (32.5 mg, 243 µmol, 6 equiv) and then heated under vacuum to 120 °C for 10 min. The solid was then cooled to r.t. and flushed with argon. Then compound **29** (25.0 mg, 40.5 µmol, 1 equiv) was added followed by dry DMPU (1.5 mL). The mixture was purged with argon in a sonicator for 30 min. The flask was then heated in a preheated oil bath (170 °C) for 20 h. The mixture was then left to cool to r.t., poured into concentrated HCl (36%) diluted with Et_2O and filtered. The collected solids were washed with 1 M HCl and dried under hv yielding **1′** (20.0 mg, 36.0 µmol, 90%).

^{1}H NMR (600 MHz, $CDCl_3$) δ: 8.91 (d, J = 2.0 Hz, 1 H), 8.74 (d, J = 2.1 Hz, 1 H), 8.31 (s, 1 H), 7.95 (s, 1 H), 7.42 (s, 1 H), 7.06 (d, J = 9.9 Hz, 1 H), 6.90 (d, J = 8.0 Hz, 2 H), 2.62 (s, 3 H), 2.54 (s, 3 H), 1.56 (s, 9 H).

^{13}C NMR (151 MHz, $CDCl_3$) δ: 182.72, 161.79, 160.16 (d, J = 8.3 Hz), 158.11 (d, J = 10.4 Hz), 157.88, 156.21, 154.34, 151.67, 143.71, 142.01, 140.22 (d, J = 8.0 Hz), 130.01, 129.83, 127.80, 125.87 – 125.84 (m), 125.32, 123.80, 123.36, 120.23, 118.15 (d, J = 2.2 Hz), 110.79 (d, J = 21.4 Hz), 110.24 (t, J = 20.6 Hz), 109.07 – 108.79 (m), 108.71 (d, J = 21.0 Hz), 105.50 (d, J = 3.6 Hz), 35.83, 31.49, 16.24, 15.49.

^{13}C{^{1}H} dept-135 NMR (151 MHz, $CDCl_3$) δ: 143.59, 129.89, 125.74, 123.24, 108.91 – 108.67 (m), 108.66, 108.52, 105.37 (d, J = 3.5 Hz), 31.36, 16.12, 15.36.

^{19}F{^{1}H} NMR (376 MHz, $CDCl_3$) δ: −110.93, −118.24.

^{19}F NMR (376 MHz, $CDCl_3$) δ: −110.93 (d, J = 7.9 Hz), −118.24 (d, J = 10.0 Hz).

HRMS (ESI) *m/z*:

Calcd. for $[C_{31}H_{23}F_3O_2S_2 + Na]^+$ 571.0976 $[M + Na]^+$; found 571.0984.

Oxophenalenoxyl 1R: Lead tetraacetate (10 g) was dissolved in glacial acetic acid (26 mL) and benzene (3 mL).

Thereafter, H_2O (10 mL) was added and the mixture was shaken for 20 min. The lead dioxide was then centrifuged and the benzene/acetic acid/water mixture was removed. The solid precipitate was then suspended in acetone, centrifuged and the acetone solution was discarded. This was repeated 5 times followed by a final suspension in toluene which was centrifuged and the toluene solution was discarded. The precipitated lead dioxide was dried over night at the hv (2×10^{-2}) and then directly used (for every experiment a new batch of lead dioxide was prepared).
An oven-dried argon flushed Schlenk tube was charged with lead dioxide (620 mg). Then a 5 mmol/L solution of **1** (5 mg, 8.79 µmol, 1 equiv) in dry toluene (1.76 mL) was added and the mixture was then stirred for 1 h under argon at r.t. The mixture was then filtered under argon. The toluene solution was directly used for the EPR and UV-Vis experiments as concentration of the solution at the rotational evaporator almost quantitatively quenched the radical.
EPR (X-band): *g*-value = 2.0032.

8-(*Tert*-butyl)-2,5-bis(2,6-dimethyl-4-(methylthio)phenyl)-6-hydroxy-1*H*-phenalen-1-one 2: A round bottom flask was charged with LiI (10.3 mg, 76.6 µmol, 2.3 equiv) and then heated under vacuum to 120 °C for 10 min. The solid was then cooled to r.t. and flushed with argon. Then compound **30** (20.0 mg, 33.3 µmol, 1 equiv) was added, followed by addition of dry DMPU (1 mL). The mixture was purged with argon in a sonicator for 30 min. The flask was then heated in a preheated oil bath (170 °C) for 18 h. The mixture was then left to cool to r.t., and then poured into 6 M HCl (36%). The mixture was extracted with distilled (to remove the BHT stabiliser) Et_2O (two times). The combined organic phase was then washed with water and brine, dried over anhydrous Na_2SO_4, filtered and concentrated under reduced pressure. The crude was further purified by reverse phase column chromatography on C^{18}-functionalised silica gel (CH_3CN : H_2O 10 : 1 + 0.1% formic acid) yielding **2** as an orange amorphous solid (16 mg, 28.9 µmol, 87%).
^{1}H NMR (500 MHz, $CDCl_3$) δ: 8.87 (d, J = 2.0 Hz, 1 H), 8.66 (d, J = 2.0 Hz, 1 H), 7.47 (s, 1 H), 7.35 (s, 1 H), 7.13 (s, 1 H), 7.04 (s, 1 H), 2.55 (s, 3 H), 2.51 (s, 3 H), 2.18 (s, 6 H), 2.11 (s, 6 H), 1.53 (s, 9 H).
^{13}C NMR (126 MHz, $CDCl_3$) δ: 183.96, 152.46, 152.19 (extracted by HMBC and HMQC), 150.36, 141.04, 139.96, 139.10, 137.67, 137.25, 137.05, 134.34 (extracted by HMBC and HMQC), 133.19, 130.21, 129.70, 126.65, 125.93, 125.78, 125.21, 123.50, 121.40, 120.67, 35.75, 31.59, 20.78, 20.68, 16.10, 15.48.
HRMS (ESI) *m/z*:
calcd. for $[C_{35}H_{36}O_2S_2\text{-}H_2O + Na]^+$ 575.2053 $[M + Na]^+$;
found 575.2049

Oxophenalenoxyl 2R: Lead tetraacetate (10 g) was dissolved in glacial acetic acid (26 mL) and benzene (3 mL). Thereafter H_2O (10 mL) was added and the mixture was shaken for 20 min. The lead dioxide was then centrifuged and the benzene acetic acid water mixture was removed. The solid precipitate was then suspended in acetone, centrifuged and the acetone solution was discarded. This was repeated 5 times followed by a final suspension in toluene which was centrifuged and the toluene solution was discarded. Precipitated lead dioxide was dried overnight at the hv (2×10^{-2}) and then directly used (for every experiment, a new batch of lead dioxide was prepared).
An oven-dried argon flushed Schlenk tube was charged with lead dioxide (620 mg). Then a 5 mM solution of **2** (1 mg, 1.81 µmol, 1equiv) in fresh distilled toluene (0.36 mL) was added and the mixture was then stirred for 1 h under argon at r.t. The mixture was then filtered under argon. The toluene solution was directly used for the EPR and UV-Vis experiments as concentration of the solution at the rotational evaporator almost quantitatively quenched the radical.
EPR (X-band): *g*-value = 2.0031.

8-(*Tert*-butyl)-6-hydroxy-2,5-diphenyl-1*H*-phenalen-1-one 3: A round bottom flask was charged with LiI (17.7 mg, 133 µmol, 6 equiv) and then heated under vacuum to 120 °C for 10 min. The solid was then cooled to r.t. and flushed with argon. Then compound **31** (10.0 mg, 22.1 µmol, 1 equiv) was added followed by dry DMPU (1.1 mL). The mixture was purged with argon in a sonicator for 30 min. The flask was then heated in a preheated oil bath (170 °C) for 18 h. The mixture was then left to cool to r.t., and then poured into concentrated HCl (36%). The mixture was extracted with distilled (to remove the BHT stabiliser) Et_2O (two times). The combined organic phase was then washed with water and brine, dried over anhydrous Na_2SO_4, filtered and concentrated under reduced pressure. The crude was further purified by reverse phase column chromatography on C^{18}-functionalised silica gel (CH_3CN : H_2O 10 : 1 + 0.1% formic acid) yielding **3** as an orange amorphous solid (3 mg, 7.42 µmol, 34%).
HPLC-grade TFA (50 µL) was added to the NMR spectrum to push the compound into a well-defined protonation state.
^{1}H NMR (600 MHz, $CDCl_3$) δ: 10.40 (s, 1 H, TFA), 9.05 (s, 2 H), 8.01 (s, 2 H), 7.56 (m, 8 H), 7.53 – 7.46 (m, 2 H), 1.55 (s, 9 H).
^{13}C NMR (151 MHz, $CDCl_3$) δ: 170.26, 160.68 (q, J = 44.1, 42.3 Hz (TFA)), 151.80, 142.13, 135.10, 132.26, 130.61, 129.66, 129.32, 129.13, 125.09, 120.70, 114.47 (q, J = 285.0 Hz (TFA)), 35.89, 31.39.
^{13}C{^{1}H} dept-135 NMR (151 MHz, $CDCl_3$) δ: 141.87, 132.02, 129.51, 129.19, 128.99, 31.25.
^{19}F NMR (565 MHz, $CDCl_3$) δ: −75.70 (TFA).
HRMS (ESI) *m/z*:
Calcd. for $[C_{29}H_{24}O_2 + H]^+$ 405.1843 $[M + H]^+$;
found 405.1849
$[C_{29}H_{24}O_2 + Na]^+$ 427.1660 $[2\,M + Na]^+$;
found 427.1669.

8-(*Tert*-butyl)-2,5-bis(4-(*tert*-butyl)phenyl)-6-hydroxy-1*H*-phenalen-1-one 4: A round bottom flask was charged with LiI (47.4 mg, 354 µmol, 20 equiv) and then heated under vacuum to 120 °C for 10 min. The solid was then cooled to r.t. and flushed with argon. Then compound **32** (10.0 mg, 17.7 µmol, 1 equiv) was added followed by dry DMPU (1.5 mL). The mixture was purged with argon in a sonicator for 30 min. The flask was then heated in a preheated oil bath (170 °C) for 18 h. The mixture was then left to cool to r.t., and then poured into aq. 6 M HCl. The mixture was extracted with distilled (to remove the BHT stabiliser) Et_2O (two times). The combined organic phase was then washed with water and brine, dried over anhydrous Na_2SO_4, filtered and concentrated under reduced pressure. The crude was further purified by column chromatography on silica gel (chloroform : pentane 8 : 1 + 0.1% formic acid) followed by GPC ($CHCl_3$) yielding **4** as an orange amorphous solid (4 mg, 7.74 µmol, 44%).

^{1}H NMR (600 MHz, $CDCl_3$) δ: 8.89 (s, 1 H), 8.67 (s, 1 H), 7.78 (s, 1 H), 7.68 – 7.59 (m, 5 H), 7.56 – 7.44 (m, 4 H), 6.33 (s, 1 H), 1.52 (s, 9 H), 1.41 (s, 9 H), 1.37 (s, 9 H).

^{13}C NMR (151 MHz, $CDCl_3$) δ: 184.31,152.29, 151.98, 150.70, 150.35, 139.37, 136.85, 134.35, 133.49, 132.90, 130.15, 129.94, 129.02, 128.80, 127.13, 126.13, 125.24, 125.17, 123.58, 122.79, 121.28, 35.72, 34.96, 34.76, 31.59, 31.52, 31.46.

^{13}C{^{1}H} dept-135 NMR (151 MHz, $CDCl_3$) δ: 139.24, 133.36, 130.01, 128.89, 128.67, 127.00, 125.11, 125.04, 31.46, 31.39, 31.34.

HRMS (ESI) *m*/*z*:

Calcd. for $[C_{37}H_{40}O_2 + H]^+$ 517.3092 $[M + H]^+$;
found 517.3101
$[C_{37}H_{40}O_2 + Na]^+$ 539.2915 $[M + Na]^+$;
found 539.2921
$[C_{37}H_{40}O_2 + K]^+$ 555.2652 $[M + K]^+$;
found 555.2660
$[C_{74}H_{80}O_4 + Na]^+$ 1055.5957 $[2\,M + Na]^+$;
found 1055.5949.

8-(*Tert*-butyl)-2,5-bis(4-fluorophenyl)-6-hydroxy-1*H*-phenalen-1-one 5: A round bottom flask was charged with LiI (41.1 mg, 307 µmol, 6 equiv) and then heated under vacuum to 120 °C for 10 min. The solid was then cooled to r.t. and flushed with argon. Then compound **33** (25.0 mg, 51.2 µmol, 1 equiv) was added followed by dry DMPU (1.5 mL). The mixture was purged with argon in a sonicator for 30 min. The flask was then heated in a preheated oil bath (170 °C) for 18 h. The mixture was then left to cool to r.t. and poured into aq. 6 M HCl. The mixture was extracted with distilled (to remove the BHT stabiliser) Et_2O (two times). The combined organic phase was then washed with water and brine, dried over anhydrous Na_2SO_4, filtered and concentrated under reduced pressure. The crude was further purified by reverse phase column chromatography on C^{18}-functionalised silica gel (CH_3CN : H_2O 10 : 1 + 1% formic acid) yielding **5** as an orange amorphous solid (9 mg, 20.4 µmol, 40%).

HPLC TFA (75 µL) was added to the NMR spectrum to push the compound into a well-defined protonation state.

^{1}H NMR (600 MHz, $CDCl_3$) δ: 10.01 (s, 1 H (TFA)), 8.95 (s, 2 H), 7.87 (s, 2 H), 7.55 (t, J = 6.8 Hz, 4 H), 7.24 (t, J = 8.3 Hz, 4 H), 1.53 (s, 9 H).

^{1}H{^{19}F} NMR (600 MHz, $CDCl_3$) δ: 10.03 (s, 1 H (TFA)), 8.95 (s, 2 H), 7.87 (s, 2 H), 7.55 (d, J = 8.4 Hz, 4 H), 7.24 (d, J = 8.0 Hz, 4 H), 1.53 (s, 9 H).

^{13}C NMR (151 MHz, $CDCl_3$) δ: 170.30, 163.96, 162.31, 160.58 (q, J = 42.2, 40.6 Hz (TFA)), 151.51, 140.47, 131.51, 131.25 (d, J = 8.3 Hz), 131.08, 129.64, 125.96, 125.49, 120.58, 116.56 (d, J = 21.8 Hz), 114.43 (q, J = 285.0 Hz (TFA)), 35.84, 31.41.

^{13}C{^{1}H} dept-135 NMR (151 MHz, $CDCl_3$) δ: 140.29, 131.11 (d, J = 8.2 Hz), 130.91, 116.42 (d, J = 21.6 Hz), 31.27.

^{19}F NMR (376 MHz, $CDCl_3$) δ: −75.57 (TFA), −112.72.

HRMS (ESI) *m*/*z*:

Calcd. for $[C_{29}H_{22}F_2O_2 - H]^-$ 439.1523 $[M - H]^-$;
found 439.1515.

3,6-Dibromonaphthalene-2,7-diol: A three-necked 250 mL round bottom flask equipped with a reflux condenser and a dropping funnel was charged with naphthalene-2,7-diole **6** (2.00 g, 12.5 mmol, 1.00 equiv) dissolved in acetic acid (46 mL). Then bromine (2.58 mL, 50.1 mmol, 4.01 equiv) in acetic acid (15 mL) was added dropwise followed by water (6.2 mL). The mixture was refluxed for 4 h and cooled to r.t. over 14 h. Then tin powder (2.60 g, 21.9 mmol, 1.75 equiv) was added and the mixture was refluxed for 2 h. Then more tin powder (742 mg, 6.25 mmol, 0.5 equiv) was added and the mixture was again refluxed for 15 h. The hot solution was filtered to remove the tin residue. The filtrate was then diluted with water (750 mL) and left standing in the fridge for 15 h. The solids were filtered off, washed with water and dried under reduced pressure yielding **7** as a white amorphous solid (2.88 g, 9.07 mmol, 73%).

The obtained analytical data matched previously reported data.[86]

^{1}H NMR (400 MHz, acetone-d_6) δ: 9.15 (s, 2 H), 8.02 (s, 2 H), 7.18 (s, 2 H).

^{13}C NMR (101 MHz, acetone-d_6) δ: 152.25, 134.71, 131.00, 125.13, 110.09, 108.61.

2,7-Dibromo-3,6-dimethoxynaphthalene 8: An oven-dried argon flushed round bottom flask was charged with 3,6-dibromonaphthalene-2,7-diol **7** (1.00 g, 3.15 mmol, 1 equiv) and K_2CO_3 (2.18 g, 15.8 mmol, 5 equiv). The flask was purged with argon. Then dry acetone (10 mL) followed by MeI (0.981 mL, 15.8 mmol, 5 equiv) were added. The reaction mixture was then stirred 19 h at r.t. Thereafter, aq. NH_4OH was added to quench the reaction. The reaction mixture was extracted with DCM (two times). The combined or-

ganic phase was washed with water and brine, dried over anhydrous Mg_2SO_4, filtered and concentrated under reduced pressure. The crude was further purified by column chromatography on silica gel (cyclohexane : DCM 4 : 1) yielding compound **8** (1.09 g, 3.15 mmol, 100%) as a white amorphous solid.

The obtained analytical data matched previously reported data.[87]

^{1}H NMR (400 MHz, $CDCl_3$) δ: 7.89 (s, 2 H), 7.06 (s, 2 H), 3.99 (s, 6 H).

^{13}C NMR (101 MHz, $CDCl_3$) δ: 154.47, 134.06, 131.17, 125.44, 111.56, 105.88, 56.37.

3,6-Dibromo-2,7-dimethoxy-1-naphthaldehyde 9: An oven-dried argon flushed round bottom flask was charged with compound **8** (500 mg, 1.45 mmol, 1 equiv) and dry DCM (30 mL). The mixture was then degassed for 10 min with argon and then cooled to −20 °C. Then $TiCl_4$ (0.165 mL, 1.45 mmol, 1equiv) was added slowly followed by the dropwise addition of dichloromethyl methyl ether (0.147 mL, 97% pure, 1.60 mmol, 1.1 equiv). The mixture was then left to warm up to r. t. over 15 h. The reaction was quenched with aq. 1 M HCl (30 mL). The organic phase was separated and the aqueous phase was extracted with DCM (two times). The combined organic phase was then washed with aq. sat. $NaHCO_3$ and water, dried over anhydrous Mg_2SO_4, filtered and concentrated under reduced pressure. The crude product was further purified by column chromatography on silica gel (cyclohexane : DCM 2 : 1) yielding compound **9** as a white solid (400 mg, 1.07 mmol, 74%).

^{1}H NMR (500 MHz, $CDCl_3$) δ: 10.75 (s, 1 H), 8.80 (s, 1 H), 8.18 (s, 1 H), 7.95 (s, 1 H), 4.06 (d, J = 1.4 Hz, 7 H).

^{13}C NMR (126 MHz, $CDCl_3$) δ: 192.10(C17), 163.16(C9), 157.24(C1), 138.75(C3), 131.53(C3), 131.31(C7), 127.85(C5), 122.98(C6), 114.47(C8), 114.40(C2), 104.92(C10), 64.57 (C13), 56.67(C14).

HRMS (ESI) m/z:

Calcd. for $[C_{13}H_{10}Br_2O_3 + Na]^+$ 394.8885 $[M + Na]^+$;
found 394.8889.

Methyl 2-(3,6-dibromo-2,7-dimethoxy-1-naphthoyl)-3,3-dimethylbutanoate 10: An oven-dried argon flushed two-necked round bottom flask was charged with dry THF (20 mL) and dry diisopropylamine (2.82 mL, 20.1 mmol, 15 equiv). This mixture was bubbled with argon for 10 min and cooled to 0 °C. Then *n*-BuLi (7.50 mL, 2.5 M in *n*-hexane, 18.8 mmol, 14 equiv) was added dropwise and the mixture was stirred for 1 h at 0 °C. Thereafter, methyl *tert*-butylacetate (2.91 mL, 19.4 mmol, 14.5 equiv) was added and the mixture was stirred for 30 min. Then 3,6-dibromo-2,7-dimethoxy-1-naphthaldehyde **9** (601 mg, 1.61 mmol, 1 equiv) dissolved in dry THF (20 mL) was added dropwise over 25 min. The mixture was stirred for 40 min at 0 °C. The reaction was quenched with 1 M HCl (20 mL) and extracted with EtOAc (two times). The combined organic phase was dried over Mg_2SO_4, filtered and concentrated under reduced pressure. The crude mixture was further purified by column chromatography on silica gel (toluene : ethyl acetate 30 : 1) yielding **10** as an off-white amorphous solid (738 mg, 1.46 mmol, 91%).

^{1}H NMR (500 MHz, $CDCl_3$) δ: 7.91 (s, 1 H), 7.88 (s, 1 H), 7.78 (s, 1 H), 5.87 (dd, J = 7.8, 4.9 Hz, 1 H), 4.02 (s, 3 H), 3.96 (s, 3 H), 3.73 (s, 3 H), 3.25 (d, J = 7.8 Hz, 1 H), 3.15 (d, J = 5.3 Hz, 1 H), 0.88 (s, 9 H).

^{13}C NMR (126 MHz, $CDCl_3$) δ: 174.85, 154.02, 153.13, 132.14, 132.03, 131.48, 128.46, 115.17, 113.36, 105.10, 67.91, 62.48, 60.77, 56.40, 51.56, 33.53, 28.35.

HRMS (ESI) m/z:

Calcd. for $[C_{20}H_{24}Br_2O_5 + Na]^+$ 524.9879 $[M + Na]^+$;
found 524.9883
$[C_{40}H_{48}Br_4O_{10} + Na]^+$ 1026.9864 $[2\,M + Na]^+$;
found 1026.9876.

Methyl 2-((3,6-dibromo-2,7-dimethoxynaphthalen-1-yl) methyl)-3,3-dimethylbutanoate 11: An oven-dried argon-flushed round bottom flask was charged with compound **10** (1.20 g, 2.38 mmol, 1 equiv) dissolved in dry DCM (9 mL) and triethylsilane (1.24 mL, 7.73 mmol, 3.25 equiv). To this mixture was added trifluoroacetic acid (1.69 mL, 22.6 mmol, 9.5 equiv). The mixture was then stirred at r. t. for 20 h. The reaction mixture was then diluted with water and the organic phase was separated. The aqueous phase was then extracted with DCM (tow times). The combined organic phase was dried over anhydrous Mg_2SO_4, filtered and concentrated under reduced pressure. The crude was further purified by column chromatography on silica gel (cyclohexane: EtOAc = 6:1) yielding compound **11** as an off-white amorphous solid (1.03 g, 2.11 mmol, 89%).

^{1}H NMR (500 MHz, $CDCl_3$) δ: 7.87 (s, 1 H), 7.80 (s, 1 H), 7.37 (s, 1 H), 4.05 (s, 3 H), 3.90 (s, 3 H), 3.38 (dd, J = 13.6, 11.2 Hz, 1H), 3.29 (s, 3 H), 3.17 (dd, J = 13.7, 2.5 Hz, 1 H), 2.57 (dd, J = 11.2, 2.5 Hz, 1 H), 1.15 (s, 9 H).

^{13}C NMR (126 MHz, $CDCl_3$) δ: 175.97, 154.08, 153.38, 132.70, 131.65, 130.28, 129.49, 127.85, 115.09, 113.09, 104.29, 61.06, 56.46, 56.29, 51.18, 33.79, 27.65, 25.65.

^{13}C{^{1}H} dept-135 NMR (126 MHz, $CDCl_3$) δ: 131.51, 130.14, 104.15, 60.92, 56.32, 56.15, 51.05, 27.51, 25.51.

HRMS (ESI) m/z:

Calcd. for $[C_{20}H_{24}Br_2O_4 + Na]^+$ 508.9936 $[M + Na]^+$;
found 508.9934
$[C_{40}H_{48}Br_4O_8 + Na]^+$ 994.9970 $[2\,M + Na]^+$;
found 994.9975.

2-((3,6-Dibromo-2,7-dimethoxynaphthalen-1-yl)methyl)-3,3-dimethylbutanoic acid 12: A round bottom flask was charged with methyl 2-((3,6-dibromo-2,7-dimethoxynaphthalen-1-yl)methyl)-3,3-dimethylbutanoate **11** (166 mg, 331 µmol, 1 equiv) dissolved in ethylene glycol

(10 mL). To this mixture was added KOH (328 mg, 85%, 4.97 mmol, 15 equiv) in one portion. The mixture was heated to 150 °C for 15 h. The mixture was then cooled to r.t., acidified with 1 M HCl and extracted with DCM (two times). The combined organic phase was washed with brine, dried over anhydrous Na_2SO_4 and concentrated under reduced pressure. The crude was further purified by reverse phase column chromatography on C^{18}-functionalised silica gel (acetonitrile : water 5 : 1 + 0.1% formic acid) yielding **12** as an off-white amorphous solid (60.0 mg, 127 µm, 38%).

^{1}H NMR (400 MHz, $CDCl_3$) δ: 7.85 (s, 1 H), 7.81 (s, 1 H), 7.31 (s, 1 H), 3.89 (s, 3 H), 3.88 (s, 3 H), 3.34 (dd, J = 13.7, 11.1 Hz, 1 H), 3.13 (dd, J = 13.7, 2.7 Hz, 1 H), 2.60 (dd, J = 11.1, 2.6 Hz, 1 H), 1.11 (s, 9 H).

HRMS (ESI) m/z:

Calcd. for $[C_{19}H_{22}Br_2O_4 - H]^-$ 470.9812 $[M - H]^-$;
found 470.9813.

5,8-Dibromo-2-(*tert*-butyl)-4,9-dimethoxy-2,3-dihydro-1*H*-phenalen-1-one 14 and side product 13: An oven-dried argon-flushed Schlenk tube was charged with triflic acid (10 mL). Compound **11** (200 mg, 0.41 mmol, 1 equiv) dissolved in dry DCM (1.5 mL) was added dropwise to the TfOH. The reaction mixture was then stirred at r.t. for 2.5 h. The reaction mixture was then poured into ice water and extracted with DCM (three times). The combined organic phase was washed with aq. sat. $NaHCO_3$, dried over anhydrous Mg_2SO_4, filtered and concentrated under reduced pressure. The crude was further purified by column chromatography on silica gel (EtOAc : toluene : cyclo 1 : 1 : 5) yielding **14** as a thick yellow oil (171 mg, 0.375 mmol, 91%). The product was used without further purification. For analytic purposes the crude was further purified by HPLC with reverse phase column chromatography on C^{18}-functionalised silica gel (gradient from 75% acetonitrile:25% H_2O with 0.1% formic acid to 95% acetonitrile:5% H_2O with 0.1% formic acid).

Compound **14**

^{1}H NMR (500 MHz, $CDCl_3$) δ: 8.10 (d, J = 0.5 Hz, 1 H), 7.87 (q, J = 0.7 Hz, 1 H), 4.02 (s, 3 H), 3.91 (s, 3 H), 3.56 (ddd, J = 17.0, 6.2, 0.8 Hz, 1 H), 3.40 (ddd, J = 17.0, 8.0, 0.8 Hz, 1 H), 2.72 (dd, J = 8.0, 6.2 Hz, 1 H), 1.01 (s, 9 H).

^{13}C NMR (126 MHz, $CDCl_3$) δ: 198.90(C11), 154.21(C10), 152.27(C6), 135.42(C7), 132.73(C5), 129.41(C3), 128.78(C4), 127.09(C2), 125.07(C8), 119.55(C9), 117.85(C1), 63.27(C23), 60.89(C24), 57.63(C12)), 33.19(C19), 28.17(C20, C21, C22), 25.85(C13).

^{13}C{^{1}H} dept-135 NMR (126 MHz, $CDCl_3$) δ: 135.27(C7), 129.26(C3), 63.13(C23), 60.75(C24), 57.49(C12), 28.03(C20, C21, C22), 25.85((C31) negative peak).

Compound **13**

^{1}H NMR (500 MHz, $CDCl_3$) δ: 8.53 (s, 1 H), 7.52 (s, 1 H), 4.02 (s, 3 H), 3.98 (s, 3 H), 3.40 (dd, J = 17.3, 6.5 Hz, 1 H), 3.17 (dd, J = 17.3, 8.4 Hz, 1 H), 2.70 (dd, J = 8.4, 6.5 Hz, 1 H), 1.02 (s, 9 H).

^{13}C NMR (126 MHz, $CDCl_3$) δ: 199.58(C11), 154.70(C9), 154.32(C1), 135.83(C7), 134.13(C10), 124.85(C8), 124.79(C4), 120.04(C5), 118.77(C6), 118.26(C3), 117.11(C2), 63.34(C22), 57.32(C12), 56.53(C23), 33.06(C18), 28.14(C19, C20, C21), 24.83(C13).

^{13}C{^{1}H} dept-135 NMR (126 MHz, $CDCl_3$) δ: 135.68, 116.96, 63.20, 57.18, 56.38, 29.85 (negative peak), 27.99, 24.83 (negative peak).

Compound **14:**

HRMS (ESI) m/z:

Calcd. for $[C_{19}H_{20}Br_2O_3 + H]^+$ 454.9846 $[M + H]^+$;
found 454.9852
$[C_{19}H_{20}Br_2O_3 + Na]^+$ 476.995 $[M + Na]^+$;
found 476.9671
$[C_{38}H_{40}Br_4O_6 + Na]^+$ 930.9456 $[M + Na]^+$;
found 930.9451.

5,8-Dibromo-2-(*tert*-butyl)-9-hydroxy-4-methoxy-2,3-dihydro-1*H*-phenalen-1-one 15: A three-necked argon-flushed oven-dried round bottom flask was charged 2-((3,6-dibromo-2,7-dimethoxynaphthalen-1-yl)methyl)-3,3-dimethylbutanoic acid **12** (100 mg, 211 µmol, 1 equiv) and oxalyl chloride (3 mL, 31.7 mmol, 150 equiv). The mixture was then stirred at 65 °C for 3 h and then cooled to r.t. The remaining oxalyl chloride was then removed by distillation under reduced pressure. Then dry DCM (1.5 mL) was added to the crude intermediate. The mixture was then again concentrated under reduced pressure and the crude intermediate was cooled to −78 °C and dry DCM (3 mL) was added followed by $AlCl_3$ (118 mg, 889 µmol, 4.2 equiv). The mixture was then stirred for 1.5 h and left to warm up to r.t. over 10 h. The reaction was then quenched with 2 M HCl and extracted with DCM (two times). The combined organic phase was washed with water and brine, dried over anhydrous Na_2SO_4, filtered and concentrated under reduced pressure. The crude was further purified by reverse phase column chromatography on C^{18}-functionalised silica gel (10 : 1, acetonitrile : water) yielding **15** as a yellow amorphous solid (30.0 mg, 67.9 µmol, 32%).

^{1}H NMR (600 MHz, $CDCl_3$) δ: 8.05 (s, 1 H, H-C7), 7.81 (s, 1 H, H-C3), 5.91 (s, 1 H, H–O-C1), 4.02 (s, 3 H, H3-C20), 3.52 – 3.45 (m, 1 H, H-C13), 3.37 – 3.30 (m, 1 H, H-C13), 2.72 (dd, J = 7.9, 6.5 Hz, 1 H, H-C12), 1.01 (s, 9 H, 3H-(C15, C16, C17)).

^{13}C NMR (151 MHz, $CDCl_3$) δ: 199.27(C11), 154.43(C9), 147.14(C1), 135.44(C7), 133.21(C5), 127.82(C3), 126.63(C8), 124.59(C2), 117.67 (C6), 117.63(C4), 112.90(C10), 63.21(C20), 57.30(C12), 33.19(C14), 28.17(C15, C16, C17), 25.66(C13).

^{13}C NMR (151 MHz, $CDCl_3$) δ: 135.31(C7), 127.70(C3), 63.09(C20), 57.17(C12), 28.05(C15, C16, C17), 25.53(C13).

HRMS (ESI) m/z:

Calcd. for $[C_{18}H_{18}Br_2O_3 - H]^-$ 440.9530 $[M - H]^-$;
found 440.9524.

2,6-Dimethyl-4-thiocyanatoaniline 17: A 100 mL round bottom flask was charged with wet SiO_2 (50% w = w, w = 8.2 g) and DCM (35.0 mL). To this was added trichloroisocyanuric acid (1.92 g, 8.24 mmol,1 equiv) and ammonium thiocyanate (627 mg, 8.24 mmol. 1 equiv) followed by 2,6-dimethylaniline **16** (1.00 g, 8.17 mmol, 1 equiv). The mixture was then stirred under air at r.t. for 45 min, filtered, concentrated to a volume of 2 mL and further purified by column chromatography on silica gel (DCM), yielding **17** as a clear amorphous solid (709 mg, 3.98 mmol, 48%).
The obtained analytical data matched previously reported literature.[65]
^{1}H NMR (500 MHz, $CDCl_3$) δ: 7.17 (p, J = 0.7 Hz, 2 H), 3.83 (s, 2 H), 2.17 (t, J = 0.7 Hz, 6 H).
^{13}C{^{1}H} dept-135 NMR (126 MHz, $CDCl_3$) δ: 132.86, 17.45.
^{13}C NMR (126 MHz, $CDCl_3$) δ: 145.35, 132.99, 123.29, 112.79, 108.84, 17.59.

2,6-Dimethyl-4-(methylthio)aniline 18: An argon-flushed round bottom flask was charged with 2,6-dimethyl-4-thiocyanatoaniline **17** (1.90 g, 10.1 mmol, 1 equiv) and EtOH (38 mL). The solution was degassed for 15 min. Then a solution of Na_2S nonahydrate (7.28 g, 30.3 mmol, 3 equiv) in water (6.6 mL) was added. The mixture was stirred at 50 °C for 2 h. The mixture was cooled over 10 min. Then a solution of degassed EtOH (6 mL) and MeI (0.943 mL, 15.2 mmol, 1.5 equiv) was added. The mixture was stirred for 3 h at r.t., quenched with aq. NH_4OH and extracted with EtOAc (two times). The combined organic phase was washed with water and brine, dried over Na_2SO_4, filtered and concentrated under reduced pressure yielding **18** as a red oil (1.40 g, 8.37 mmol, 83%).
The obtained analytical data matched previously reported literature.[88,89]
^{1}H NMR (500 MHz, $CDCl_3$) δ: 7.00 (s, 2 H), 3.57 (s, 2 H), 2.41 (s, 3 H), 2.16 (s, 6 H).
^{13}C NMR (126 MHz, $CDCl_3$) δ: 141.77, 130.16, 124.96, 122.62, 19.13, 17.69.
^{13}C{^{1}H} dept-135 NMR (126 MHz, $CDCl_3$) δ: 130.03, 19.00, 17.56.

2-(2,6-Dimethyl-4-(methylthio)phenyl)-4,4,5,5-tetramethyl-1,3,2-dioxaborolane 19: A round bottom flask equipped with a reflux condenser was charged with B_2Pin_2 (668 mg, 2.63 mmol, 1.1 equiv) and the 2,6-dimethyl-4-(methylthio)aniline **18** (400 mg, 2.39 mmol, 1 equiv). The solids were purged with argon. Then dry acetonitrile (7.2 mL) was added and the solution was purged with argon for 15 min. Thereafter, *tert*-butyl nitrite (0.48 mL, 90%, 3.59 mmol, 1.5 equiv) was added at once. The mixture was stirred for 9 h at reflux, cooled to r.t. and concentrated under reduced pressure. The crude was further purified by column chromatography on silica gel (cyclohexane : DCM 1 : 1) yielding **19** as a yellow solid (107 mg, 358 µmol, 16%).
^{1}H NMR (500 MHz, $CDCl_3$) δ: 6.84 (p, J = 0.6 Hz, 2 H), 2.44 (s, 3 H), 2.38 (t, J = 0.6 Hz, 6 H), 1.37 (s, 12 H).
^{13}C NMR (126 MHz, $CDCl_3$) δ: 142.95, 139.59 (extracted from HMBC and HMQC), 124.51, 83.75, 25.09, 22.46, 15.49.
^{13}C{^{1}H} dept-135 NMR (126 MHz, $CDCl_3$) δ: 24.95, 22.32, 15.35.

(3,5-Difluorophenyl)(methyl)sulfane 21: A round bottom flask was charged with 3,5-difluorobenzenethiol **20** (5.00 g, 34.2 mmol, 1 equiv) and K_2CO_3 (28.4 g, 205 mmol, 6 equiv) and acetonitrile (50 mL). To this was added MeI (3.19 mL, 51.3 mmol, 1.5 equiv). The reaction mixture was stirred for 16 h at r.t. Then aq. NH_4OH was added to quench the reaction. The mixture was then extracted with TBME (two times). The combined organic phase was then washed with 1 M NaOH, water and brine, dried over anhydrous Na_2SO_4, filtered and concentrated under reduced pressure. The crude was plugged over silica gel ($CHCl_3$) yielding **21** as a clear colourless oil (5.48 g, 34.2 mmol, quant.).
The obtained analytical data matched previously reported literature.[90]
^{1}H NMR (400 MHz, $CDCl_3$) δ: 6.79 – 6.66 (m, 1 H), 6.61 – 6.51 (m, 1 H), 2.48 (s, 2 H).
^{1}H{^{19}F} NMR (400 MHz, $CDCl_3$) δ: 6.73 (d, J = 2.2 Hz, 1 H), 6.56 (t, J = 2.3 Hz, 1 H), 2.48 (s, 2 H).
^{19}F NMR (376 MHz, $CDCl_3$) δ: −108.89 to −110.69 (m).
^{19}F{^{1}H} NMR (376 MHz, $CDCl_3$) δ: −109.69.
^{13}C NMR (101 MHz, $CDCl_3$) δ: 163.29 (dd, J = 249.5, 13.4 Hz), 142.92 (d, J = 10.0 Hz), 109.30 – 108.02 (m), 100.44 (t, J = 25.6 Hz), 15.39.

2-(2,6-Difluoro-4-(methylthio)phenyl)-4,4,5,5-tetramethyl-1,3,2-dioxaborolane 22: An oven-dried argon-flushed round bottom flask was charged with (3,5-difluorophenyl)(methyl)sulfane **21** (2.00 g, 12.0. mmol, 1 equiv). To this was added dry THF (63 mL). The solution was bubbled with argon for 15 min and cooled to −78 °C. Then *n*-BuLi (5.00 mL, 2.5 M in hexane, 12.5 mmol, 1 equiv) was added dropwise. The mixture was then stirred at −78 °C for 2 h. Then 2-isopropoxy-4,4,5,5-tetramethyl-1,3,2-dioxaborolane (3.06 mL, 15 mmol 1.2 equiv) was added dropwise and then the mixture was left to warm up to r.t. over 16 h. Upon completion of the reaction, the reaction mixture was quenched with aq. sat. $NaHCO_3$ and extracted with EtOAc (two times). The combined organic phase was washed with water and brine, dried over anhydrous Na_2SO_4, filtered and concentrated under reduced pressure yielding **22** as a clear oil (3.43 g, 12.0 mmol, 96%).
The obtained analytical data matched previously reported literature.[69]
^{1}H NMR (500 MHz, $CDCl_3$) δ: 6.72 – 6.66 (m, 1 H), 2.47 (s, 2 H), 1.37 (s, 7 H).
^{1}H{^{19}F} NMR (500 MHz, $CDCl_3$) δ: 6.69 (s, 1 H), 2.47 (s, 2 H), 1.37 (s, 8 H).

^{19}F NMR (471 MHz, $CDCl_3$) δ: −99.73 to −100.79 (m).
^{19}F{^{1}H} NMR (471 MHz, $CDCl_3$) δ: −100.15.
^{13}C NMR (126 MHz, $CDCl_3$) δ: 168.08 (d, J = 14.2 Hz), 166.07 (d, J = 14.1 Hz), 146.54 – 146.28 (m), 108.25 – 107.89 (m), 84.16, 24.89, 14.97.
^{13}C{^{1}H} dept-135 NMR (126 MHz, $CDCl_3$) δ: 107.94 (d, J = 29.3 Hz), 24.74, 14.83.

(2,6-Difluoro-4-(methylthio)phenyl)boronic acid 23: A round bottom flask was charged with the pinacol ester **22** (309 mg, 1.08 mmol, 1.0 equiv) and methylboronic acid (333 mg, 5.4 mmol, 5.0 equiv). The solids were dissolved in a mixture of acetone and 0.2 M HCl (10 mL, 1 : 1, v/v). The reaction mixture was stirred for 8 h at r.t. The mixture was concentrated under reduced pressure yielding **23** as an off-white solid (220 mg, 1.08 mmol, quant.). The crude product was considered pure enough and directly used in the next step without any further purification. For every Suzuki cross-coupling reaction in which **23** was used, a new batch was synthesized.
^{1}H NMR (400 MHz, MeOD) δ: 6.87 – 6.78 (m, 2 H), 2.50 (s, 3 H).

2-(*Tert*-butyl)-5,8-bis(2,6-difluoro-4-(methylthio)phenyl)-4,9-dimethoxy-2,3-dihydro-1*H*-phenalen-1-one 24: An oven-dried argon flushed Schlenk tube was charged with boronic acid **23** (47.0 mg, 95%, 219 µmol, 5 equiv), compound **14** (20.0 mg, 43.8 µmol, 1 equiv) and KF (30.5 mg, 526 µmol, 12 equiv). The solids were purged with argon (three times). The solids were dissolved in a degassed THF/water mixture (10 : 1 2.2 mL) and purged with argon for 10 min. Then tri-*tert*-butyl phosphine (5.69 µL, 95%, 21.9 µmol, 0.5 equiv) was added and the mixture was further degassed for 2 min. Then $Pd_2(dba)_3$ (10.0 mg, 11.0 µmol, 0.25 equiv) was added and the mixture was heated to 70 °C and stirred for 3 h. The reaction mixture was cooled to r.t., poured into an aq. sat. Na_2CO_3 and extracted with DCM (two times). The combined organic phase was dried over anhydrous Mg_2SO_4, filtered and concentrated under reduced pressure. The crude product was then further purified by column chromatography on silica gel (DCM) yielding compound **24** as a yellow amorphous solid (25.0 mg, 40.7 µmol, 93%).
^{1}H NMR (500 MHz, $CDCl_3$) δ: 7.87 (s, 1 H), 7.66 (s, 1 H), 6.93 – 6.84 (m, 4 H), 3.72 (s, 3 H), 3.68 (dd, J = 16.6, 6.0 Hz, 1 H), 3.57 (s, 3 H), 3.35 (ddd, J = 16.6, 9.8, 0.8 Hz, 1 H), 2.86 (dd, J = 9.8, 6.0 Hz, 1 H), 2.54 (s, 3 H), 2.53 (s, 3 H), 1.12 (s, 9 H).
^{1}H{^{19}F} NMR (500 MHz, $CDCl_3$) δ: 7.87 (s, 1 H), 7.66 (s, 1 H), 6.91 – 6.86 (m, 4 H), 3.72 (s, 3 H), 3.68 (dd, J = 16.7, 6.0 Hz, 1 H), 3.57 (s, 3 H), 3.41 – 3.30 (m, 1 H), 2.86 (dd, J = 9.8, 6.0 Hz, 1 H), 2.54 (s, 3 H), 2.53 (s, 3 H), 1.12 (s, 9 H).
^{19}F NMR (471 MHz, $CDCl_3$) δ: −111.28 (td, J = 7.3, 3.5 Hz), −111.54 to −111.69 (m).
^{13}C NMR (126 MHz, $CDCl_3$) δ: 199.82, 161.74 – 161.27 (m), 159.70 – 159.39 (m), 154.36, 141.96 (td, J = 10.4, 5.4 Hz), 136.05, 134.89, 129.97, 126.26, 124.96, 123.82, 123.27, 122.39, 111.14 (t, J = 21.3 Hz), 110.77 (t, J = 21.2 Hz), 108.76 – 108.30 (m), 62.90, 60.92, 57.24, 32.82, 28.05, 25.61.
HRMS (ESI) m/z:
Calcd. for $[C_{33}H_{30}F_4O_3S_2 + Na]^+$ 637.1470 $[M + Na]^+$;
found 637.1465
$[C_{33}H_{30}F_4O_3S_2 + K]^+$ 653.1201 $[M + K]^+$;
found 653.1204
$[C_{66}H_{60}F_8O_3S_4 + Na]^+$ 1251.3026 $[2\,M + Na]^+$;
found 1251.3037.

2-(*Tert*-butyl)-5,8-bis(2,6-dimethyl-4-(methylthio)phenyl)-4,9-dimethoxy-2,3-dihydro-1*H*-phenalen-1-one 25: An oven-dried argon flushed Schlenk tube was charged with pinacolborane **19** (53.5 mg, 95%, 184 µmol, 2 equiv), compound **14** (42.0 mg, 92.1 µmol, 1 equiv) and KF (64.9 mg, 1.11 mmol, 12 equiv). The solids were purged with argon (three times). The solids were dissolved in a degassed THF/water mixture (10 : 1 8.8 mL) and purged with argon for 10 min. Then tri-*tert*-butyl phosphine (0.012 mL, 95%, 46.1 µmol, 0.5 equiv) was added and the mixture was further degassed for 2 min. Then $Pd_2(dba)_3$ (21.1 mg, 23.0 µmol, 0.25 equiv) was added and the mixture was heated to 70 °C and stirred for 3 h. The reaction mixture was cooled to r.t., poured into an aq. sat. Na_2CO_3 and extracted with DCM (two times). The combined organic phase was dried over anhydrous Mg_2SO_4, filtered and concentrated under reduced pressure. The crude was then further purified by column chromatography on silica gel (DCM) yielding compound **25** as a yellow amorphous solid (25.0 mg, 41.7 µmol, 45%).
^{1}H NMR (500 MHz, $CDCl_3$) δ: 7.58 (s, 1 H), 7.35 (s, 1 H), 7.08 – 7.01 (m, 4H), 3.58 (m, 4 H), 3.45 (m, 4 H), 2.84 (dd, J = 7.8, 6.2 Hz, 1 H), 2.53 (s, 3 H), 2.52 (s, 3 H), 2.13 (s, 3 H), 2.10 (s, 3 H), 2.07 (s, 3 H), 2.06 (s, 3 H), 1.06 (s, 9 H).
^{13}C NMR (126 MHz, $CDCl_3$) δ: 200.53, 155.93, 153.67, 137.54, 137.46, 137.21, 137.17, 137.13, 134.75, 134.55, 134.33, 134.29, 133.56, 133.08, 128.10, 126.99, 125.28, 125.26, 125.21, 125.20, 124.60, 123.55, 62.00, 60.04, 57.59, 33.05, 28.18, 25.54, 21.01, 20.98, 20.80, 15.68.
HRMS (ESI) m/z:
Calcd. for $[C_{37}H_{42}O_3S_2 + H]^+$ 599.2646 $[M + H]^+$;
found 599.2648
$[C_{37}H_{42}O_3S_2 + Na]^+$ 621.2459 $[M + Na]^+$;
found 621.2468.

2-(*Tert*-butyl)-4,9-dimethoxy-5,8-diphenyl-2,3-dihydro-1*H*-phenalen-1-one 26: An oven-dried argon flushed Schlenk tube was charged with phenylboronic acid (112 mg, 875 µmol, 5 equiv), compound **14** (80 mg, 175 µmol, 1 equiv) and KF (123 mg, 2.1 mmol, 12 equiv). The solids were three times purged with argon. The solids

were dissolved in a degassed THF/water mixture (10 : 1 8.8 mL) and purged with argon for 10 min. Then tri-*tert*-butylphosphine (0.02 mL, 95%, 87.5 µmol, 0.5 equiv) was added and the mixture was further degassed for 2 min. Then $Pd_2(dba)_3$ (40 mg, 43.8 µmol, 0.25 equiv) was added and the mixture was heated to 70 °C and stirred for 3 h. The reaction mixture was cooled to r.t., poured into an aq. sat. Na_2CO_3 and extracted with DCM (two times). The combined organic phase was dried over anhydrous Mg_2SO_4, filtered and concentrated under reduced pressure. The crude was then further purified by column chromatography on silica gel (DCM) yielding compound **26** as a yellow amorphous solid (73 mg, 175 µmol, 93%).

^{1}H NMR (500 MHz, $CDCl_3$) δ: 7.93 (s, 1 H), 7.70 – 7.63 (m, 3 H), 7.50 – 7.44 (m, 2 H), 7.42 – 7.38 (m, 1 H), 3.64 (ddd, J = 16.8, 6.1, 0.6 Hz, 1 H), 3.57 (s, 3 H), 3.46 (s, 3 H), 3.42 (ddd, J = 16.9, 8.6, 0.8 Hz, 1 H), 2.83 (dd, J = 8.5, 6.1 Hz, 1 H), 1.11 (s, 9 H).

^{13}C NMR (126 MHz, $CDCl_3$) δ: 200.49, 155.64, 153.46, 138.22, 137.75, 135.73, 134.62, 134.51, 133.17, 129.46, 129.15, 128.42, 128.30, 128.18, 127.54, 127.50, 127.10, 124.85, 123.75, 62.10, 60.32, 57.71, 32.99, 28.16, 25.49.

^{13}C{^{1}H} dept-135 NMR (126 MHz, $CDCl_3$) δ: 134.51, 129.46, 129.15, 128.42, 128.30, 128.18, 127.54, 127.50, 62.10, 60.32, 57.71, 28.16, 25.49.

HRMS (ESI) *m*/*z*:
Calcd. for $[C_{31}H_{30}O_3 + H]^+$ 451.2273 $[M + H]^+$;
found 451.2268
$[C_{31}H_{30}O_3 + Na]^+$ 473.2094 $[M + Na]^+$;
found 473.2087
$[C_{62}H_{60}O_6 + Na]^+$ 923.4293 $[2\,M + Na]^+$;
found 923.4282.

2-(*Tert*-butyl)-5,8-bis(4-(*tert*-butyl)phenyl)-4,9-dimethoxy-2,3-dihydro-1*H*-phenalen-1-one 27: An oven-dried argon-flushed Schlenk tube was charged with 4-*tert*-butylphenylboronic acid (51.2 mg, 0.273 mmol, 5 equiv), compound **14** (25 mg, 54.8 µmol, 1 equiv) and KF (38.5 mg, 0.656 mmol, 12 equiv). The solids were purged with argon (three times). The solids were dissolved in a degassed THF/water mixture (10 : 1 6.6 mL) and purged with argon for 10 min. Then tri-*tert*-butylphosphine (0.007 mL, 95%, 27.4 µmol, 0.5 equiv) was added and the mixture was further degassed for 2 min. Then $Pd_2(dba)_3$ (12.5 mg, 13.7 µmol, 0.25 equiv) was added and the mixture was heated to 70 °C and stirred for 3 h. The reaction mixture was cooled to r.t., poured into an aq. sat. Na_2CO_3 and extracted with DCM (two times). The combined organic phase was dried over anhydrous Na_2SO_4, filtered and concentrated under reduced pressure. The crude was then further purified by column chromatography on silica gel (DCM) yielding compound **27** as a yellow amorphous solid (25 mg, 0.044 mmol, 81%).

^{1}H NMR (500 MHz, $CDCl_3$) δ: 7.92 (s, 1 H), 7.69 (s, 1 H), 7.63 – 7.59 (m, 4 H), 7.51 – 7.46 (m, 4 H), 3.69 – 3.63 (m, 1 H), 3.59 (s, 3 H), 3.48 (s, 3 H), 3.44 – 3.37 (m, 1 H), 2.83 (dd, J = 8.8, 6.1 Hz, 1 H), 1.40 (s, 9 H), 1.39 (s, 9 H), 1.13(s, 9 H).

^{13}C NMR (126 MHz, $CDCl_3$) δ: 200.73, 155.88, 153.68, 150.62 (d, J = 3.4 Hz), 135.60, 135.36, 134.91, 134.56, 134.54, 133.04, 129.19, 128.88, 128.19, 127.30, 125.45, 125.35, 124.83, 123.82, 62.24, 60.47, 57.83, 34.75, 33.08, 31.55, 31.54, 28.29, 25.67.

^{13}C{^{1}H} dept-135 NMR (126 MHz, $CDCl_3$) δ: 134.43, 129.06, 128.75, 128.07, 125.33, 125.22, 62.11, 60.35, 57.70, 31.42, 28.17, 25.55.

HRMS (ESI) *m*/*z*:
Calcd. for $[C_{39}H_{46}O_3 + H]^+$ 563.3521 $[M + H]^+$;
found 563.3520
$[C_{39}H_{46}O_3 + Na]^+$ 585.3341 $[M + Na]^+$;
found 585.3339.

2-(*Tert*-butyl)-5,8-bis(4-fluorophenyl)-4,9-dimethoxy-2,3-dihydro-1*H*-phenalen-1-one 28: An oven-dried argon-flushed Schlenk tube was charged with 4-fluorophenylboronic acid (30.6 mg, 219 µmol, 5 equiv), compound **14** (20 mg, 43.8 µmol, 1 equiv) and KF (30.8 mg, 524 µmol, 12 equiv). The solids were purged with argon (three times). The solids were dissolved in a degassed THF/water mixture (10 : 1 1.1 mL) and purged with argon for 10 min. Then tri-*tert*-butylphosphine (0.006 mL, 95%, 21.9 µmol, 0.5 equiv) was added and the mixture was further degassed for 2 min. Then $Pd_2(dba)_3$ (10.0 mg, 10.9 µmol, 0.25 equiv) was added and the mixture was heated to 70 °C and stirred for 3 h. The reaction mixture was cooled to r.t., poured into an aq. sat. Na_2CO_3 and extracted with DCM (two times). The combined organic phase was dried over anhydrous Mg_2SO_4, filtered and concentrated under reduced pressure. The crude was then further purified by column chromatography on silica gel (DCM : cyclohexane 15 : 1) yielding compound **28** as a yellow amorphous solid (19 mg, 39.0 µmol, 89%).

^{1}H NMR (600 MHz, $CDCl_3$) δ: 7.89 (s, 1 H), 7.66 (s, 1 H), 7.66 – 7.58 (m, 4 H), 7.20 – 7.12 (m, 4 H), 3.61 (d, J = 6.1 Hz, 1 H), 3.57 (s, 3 H), 3.45 (s, 3 H), 3.41 (dd, J = 16.8, 8.5 Hz, 1 H), 2.81 (dd, J = 8.2, 6.4 Hz, 1 H), 1.10 (s, 9 H).

^{1}H{^{19}F} NMR (600 MHz, $CDCl_3$) δ: 7.89 (s, 1 H), 7.66 (s, 1 H), 7.66 – 7.61 (m, 4 H), 7.20 – 7.12 (m, 4 H), 3.63 (dd, J = 16.8, 6.1 Hz, 1 H), 3.57 (s, 3 H), 3.45 (s, 3 H), 3.41 (dd, J = 16.8, 8.5 Hz, 1 H), 2.81 (dd, J = 8.2, 6.3 Hz, 1 H), 1.10 (s, 9 H).

^{19}F NMR (565 MHz, $CDCl_3$) δ: −114.68, −114.73.

^{13}C NMR (151 MHz, $CDCl_3$) δ: 200.53, 163.41, 161.76, 155.62, 153.47, 134.91, 134.40, 134.14 (d, J = 3.3 Hz), 133.81, 133.66 (d, J = 3.3 Hz), 133.34, 131.24 (d, J = 8.0 Hz), 130.91 (d, J = 8.0 Hz), 128.08, 127.19, 125.20, 123.92, 115.54 (d, J = 17.1 Hz), 115.40 (d, J = 17.1 Hz), 62.21, 60.39, 57.79, 33.13, 28.26, 25.56.

^{13}C{^{1}H} dept-135 NMR (151 MHz, $CDCl_3$) δ: 134.28, 131.12 (d, J = 8.0 Hz), 130.79 (d, J = 8.0 Hz), 127.97, 115.42 (d,

J = 17.3 Hz), 115.28 (d, *J* = 17.3 Hz), 62.09, 60.28, 57.68, 28.15, 25.45.

HRMS (ESI) *m/z*:

Calcd. for $[C_{31}H_{28}F_2O_3 + H]^+$ 487.2080 $[M + H]^+$;
found 487.2079
$[C_{31}H_{28}F_2O_3 + Na]^+$ 509.1905 $[M + Na]^+$;
found 509.1899
$[C_{31}H_{28}F_2O_3 + K]^+$ 525.1634 $[M + K]^+$;
found 525.1638
$[C_{62}H_{56}F_4O_6 + Na]^+$ 995.3928 $[2\,M + Na]^+$;
found 995.3905
$[C_{62}H_{56}F_4O_6 + K]^+$ 1011.3649 $[2\,M + Na]^+$;
found 1011.3645.

2-(*Tert*-butyl)-5,8-bis(2,6-difluoro-4-(methylthio)phenyl)-4,9-dimethoxy-2,3-dihydro-1*H*-phenalen-1-ol 29: An oven-dried argon-flushed two-necked round bottom flask was charged with compound **24** (62 mg, 101 µmol, 1.00 equiv) dissolved in dry THF (3 mL) and cooled to 0 °C. DIBAL-H (0.44 mL, 1 M THF, 444 µmol, 4.4 equiv) was added dropwise to this mixture. The reaction was stirred for 2 h at 0 °C, then poured into a mixture of aq. sat. NH_4Cl and aq. 1 M NaOH (1 : 1) and extracted with DCM (three times). The combined organic phase was then washed with water and brine, dried over Na_2SO_4, filtered and concentrated under reduced pressure. The crude was further purified by GPC (chloroform) yielding **29** as an off-white clear glass like solid (59 mg, 95.7 µmol, 95%).

^{1}H NMR (500 MHz, $CDCl_3$) *δ*: 7.72 (s, 1 H), 7.62 (s, 1 H), 6.89 (dd, *J* = 8.3, 2.1 Hz, 4 H), 5.73 (d, *J* = 4.1 Hz, 1 H), 3.63 (s, 3 H), 3.60 (s, 3 H), 3.38 (ddd, *J* = 16.2, 3.7, 1.3 Hz, 1 H), 3.09 (ddd, *J* = 16.2, 13.3, 1.2 Hz, 1 H), 2.54 (s, 6 H), 1.69 (ddd, *J* = 13.2, 3.6, 1.9 Hz, 1 H), 1.66 – 1.60 (m, 1 H), 1.22 (s, 9 H).

^{13}C NMR (126 MHz, $CDCl_3$) *δ*: 161.69 (d, *J* = 7.6 Hz), 159.78 – 159.58 (m), 153.72, 153.62, 141.94 (t, *J* = 10.4 Hz), 141.64 (t, *J* = 10.3 Hz), 132.24, 131.13, 129.47, 129.41,127.40, 127.39, 122.29, 122.10, 111.74 (dt, *J* = 30.0, 21.3 Hz), 108.95 – 108.65 (m), 108.60 (t, *J* = 2.4 Hz), 63.77, 62.95, 61.07, 47.88, 33.03, 28.99, 19.28, 15.42, 15.39

^{19}F NMR (471 MHz, $CDCl_3$) *δ*: −111.18 (m,), −111.26 to −111.34 (m), −111.61 (m), −111.81 (m).

^{19}F NMR (471 MHz, $CDCl_3$) cpd *δ*: −111.17 (d, *J* = 6.5 Hz), −111.30 (d, *J* = 6.7 Hz), −111.61 (d, *J* = 6.5 Hz), −111.81 (d, *J* = 6.7 Hz).

HRMS (ESI) *m/z*:

Calcd. for $[C_{33}H_{30}F_4O_2S_2\text{-}H_2O + H]^+$ 599.1696 $[M\text{-}H_2O + H]^+$;
found 599.1696
$[C_{33}H_{32}F_4O_3S_2]^+$ 616.1711 $[M]^+$;
found 616.1621
Radical cation
$[C_{33}H_{32}F_4O_3S_2 + Na]^+$ 639.1627 $[M + Na]^+$;
found 639.1621
$[C_{33}H_{32}F_4O_3S_2 + K]^+$ 655.1351 $[M + K]^+$;
found 655.1361
$[C_{66}H_{64}F_8O_6S_4 + NH_4]^+$ 1250.3800 $[2\,M + NH_4]^+$;
found 1250.3796
$[C_{66}H_{64}F_8O_6S_4 + Na]^+$ 1255.3366 $[2\,M + Na]^+$;
found 1255.3350
$[C_{66}H_{64}F_8O_6S_4 + K]^+$ 1271.3103 $[2\,M + K]^+$;
found 1271.3090.

2-(*Tert*-butyl)-5,8-bis(2,6-dimethyl-4-(methylthio)phenyl)-4,9-dimethoxy-2,3-dihydro-1*H*-phenalen-1-ol 30: An oven-dried argon-flushed two-necked round bottom flask was charged with compound **25** (25.0 mg, 41.7 µmol, 1 equiv) dissolved in dry THF (0.8 mL) and cooled to 0 °C. DIBAL-H (0.18 mL, 1 M cyclohexane, 183 µmol, 4.4 equiv) was added dropwise to this mixture. The reaction was stirred for 2 h at 0 °C, then poured into a mixture of aq. sat. NH_4Cl and aq. 1 M NaOH (1 : 1) and extracted with DCM (three times). The combined organic phase was then washed with water and brine, dried over anhydrous Na_2SO_4, filtered and concentrated under reduced pressure. The crude was further purified by column chromatography on silica gel (cyclohexane : EtOAc 5 : 1) followed by GPC (chloroform) yielding **30** as a yellowish amorphous solid (23 mg, 38.3 µmol, 92%).

^{1}H NMR (500 MHz, $CDCl_3$) *δ*: 7.41 (s, 1 H), 7.30 (s, 1 H), 7.07 – 7.03 (m, 4 H), 5.71 (s, 1 H), 3.49 (s, 3 H), 3.47 (s, 3 H), 3.38 (ddd, *J* = 16.3, 3.7, 1.3 Hz, 1 H), 3.05 (ddd, *J* = 16.4, 13.5, 1.2 Hz, 1 H), 2.53 (s, 6 H), 2.13 (s, 3 H), 2.10 (s, 3 H), 2.09 (s, 6 H), 1.72 (ddd, *J* = 13.3, 3.6, 2.1 Hz, 1 H), 1.24 (s, 9 H).

^{13}C NMR (126 MHz, $CDCl_3$) *δ*: 153.04, 152.90, 137.87, 137.64, 137.54, 137.34, 137.14, 136.85, 135.56, 135.26, 132.92, 132.44, 130.47, 129.52, 129.03, 128.02, 127.57, 127.06, 125.48, 125.45, 125.43, 125.36, 64.11, 61.62, 60.30, 47.94, 33.10, 29.01, 21.24, 21.15, 21.02, 19.22, 15.91, 15.86.

HRMS (ESI) *m/z*:

Calcd. for $[C_{37}H_{42}O_2S_2\text{-}H_2O + H]^+$ 583.2695 $[M\text{-}H_2O + H]^+$;
found 583.2699
$[C_{37}H_{44}O_3S_2]^+$ 600.2714 $[M]^+$;
found 600.2726
$[C_{37}H_{44}O_3S_2 + Na]^+$ 623.2618 $[M + Na]^+$;
found 623.2624
$[C_{37}H_{44}O_3S_2 + K]^+$ 639.2362 $[M + K]^+$;
found 639.2363
$[C_{74}H_{88}O_6S_4 + Na]^+$ 1223.5359 $[2\,M + Na]^+$;
found 1223.5356.

2-(*Tert*-butyl)-4,9-dimethoxy-5,8-diphenyl-2,3-dihydro-1*H*-phenalen-1-ol 31: An oven-dried argon-flushed two-necked round bottom flask was charged with compound **26** (68.0 mg, 151 µmol, 1 equiv) dissolved in dry THF (5 mL) and then cooled to 0 °C. DIBAL-H (1.21 mL, 1 M in cyclohexane, 1.21 mmol, 8 equiv) was added dropwise to this mixture. The reaction was stirred for 2 h at 0 °C, poured into aq. sat. NH_4Cl and extracted with DCM (three times). The combined organic phase was washed with brine and concentrated under reduced pressure. The crude mixture was further pu-

rified by GPC (chloroform) yielding **31** as a white amorphous solid (66.0 mg, 151 µmol, 97%).

^{1}H NMR (500 MHz, $CDCl_3$) δ: 7.77 (s, 1 H), 7.69 – 7.64 (m, 5 H), 7.50 – 7.43 (m, 4 H), 7.42 – 7.36 (m, 2 H), 5.77 – 5.72 (m, 1 H), 3.50 (s, 3 H), 3.48 (s, 3 H), 3.42 (ddd, J = 16.3, 3.6, 1.5 Hz, 1 H), 3.06 (ddd, J = 16.3, 13.3, 1.3 Hz, 1 H), 1.66 (ddd, J = 13.3, 3.6, 2.1 Hz, 1 H), 1.62 (d, J = 4.8 Hz, 1 H), 1.24 (s, 9 H).

^{13}C NMR (126 MHz, $CDCl_3$) δ: 152.89, 152.75, 138.93, 138.76, 134.54, 134.19, 130.46, 129.41, 129.34, 129.33, 129.25, 128.57, 128.41, 128.12, 127.74, 127.48, 127.35, 127.33, 63.97, 62.09, 60.56, 48.34, 33.07, 29.00, 19.10.

^{13}C{^{1}H} dept-135 NMR (126 MHz, $CDCl_3$) δ: 130.32, 129.27, 129.11, 128.43, 128.28, 127.60, 127.35, 127.22, 63.83, 61.95, 60.42, 48.20, 28.86, 18.96.

HRMS (ESI) *m/z*:

Calcd. for $[C_{31}H_{32}O_3 + Na]^+$ 475.2239 $[M + H]^+$;
found 475.2244
$[C_{62}H_{64}O_6 + Na]^+$ 927.4599 $[2\,M + Na]^+$;
found 927.4595.

2-(*Tert*-butyl)-5,8-bis(4-(*tert*-butyl)phenyl)-4,9-dimethoxy-2,3-dihydro-1*H*-phenalen-1-ol 32: An oven-dried argon-flushed two-necked round bottom flask was charged with compound **27** (25.0 mg, 44.4 µmol, 1 equiv) dissolved in dry THF (2 mL) and then cooled to 0 °C. DIBAL-H (0.36 mL, 1 M in cyclohexane, 355 µmol, 8 equiv) was added dropwise to this mixture. The reaction was stirred for 2 h at 0 °C, poured into aq. 1 M NaOH and extracted with DCM (three times). The combined organic phase was washed with brine and concentrated under reduced pressure. The crude mixture was further purified by GPC (chloroform) yielding **32** as a pale yellow amorphous solid (22.0 mg, 39.0 µmol, 88%).

^{1}H NMR (500 MHz, $CDCl_3$) δ: 7.77 (s, 1 H), 7.67 (s, 1 H), 7.65 – 7.59 (m, 4 H), 7.50 – 7.47 (m, 4 H), 5.76 (s, 1 H), 3.52 (s, 3 H), 3.51 (s, 3 H), 3.42 (ddd, J = 16.1, 3.6, 1.3 Hz, 1 H), 3.07 (dd, J = 15.8, 13.6 Hz, 1 H), 1.70 – 1.64 (m, 1 H), 1.40 (s, 9 H), 1.40 (s, 9 H), 1.26 (s, 9 H).

^{13}C NMR (126 MHz, $CDCl_3$) δ: 152.95, 152.83, 150.44, 150.26, 135.93, 135.76, 134.30, 133.97, 130.34, 129.22, 129.05, 128.98, 128.82, 128.18, 127.63, 127.17, 125.45, 125.31, 63.98, 62.08, 60.57, 48.35, 34.74, 33.07, 31.57, 29.01, 19.11.

^{13}C{^{1}H} dept-135 NMR (126 MHz, $CDCl_3$) δ: 130.23, 128.87, 128.70, 127.51, 125.33, 125.20, 63.86, 61.97, 60.45, 48.23, 31.45, 28.89, 19.00.

HRMS (ESI) *m/z*:

Calcd. for $[C_{39}H_{48}O_3]^+$ 564.3588 $[M]^+$;
found 564.3598
$[C_{39}H_{46}O_2 + H\text{-}H_2O]^+$ 547.3560 $[M\text{-}H_2O + H]^+$;
found 547.3571.

The observed mass 547.3571 belongs to the elimination product that occurs due to the acidic conditions during the ESI MS measurement.

2-(*Tert*-butyl)-5,8-bis(4-fluorophenyl)-4,9-dimethoxy-2,3-dihydro-1*H*-phenalen-1-ol 33: An oven-dried argon-flushed two-necked round bottom flask was charged with compound **28** (19 mg, 39.0 µmol, 1 equiv) dissolved in dry THF (0.8 mL) and then cooled to 0 °C. DIBAL-H (0.3 mL, 1 M THF, 312 µmol, 8 equiv) was added dropwise to this mixture. The reaction was stirred for 2 h at 0 °C, then poured into aq. sat. NH_4Cl and extracted with DCM (three times). The combined organic phase was then washed with brine and concentrated under reduced pressure. The crude mixture was further purified by GPC (chloroform) yielding **33** as an off-white glass like amorphous solid (19 mg, 39.0 µmol, quant.).

^{1}H NMR (600 MHz, $CDCl_3$) δ: 7.73 (s, 1 H), 7.67 – 7.60 (m, 5 H), 7.15 (m, 4 H), 5.73 (s, 1 H), 3.50 (s, 3 H), 3.47 (s, 3 H), 3.40 (ddd, J = 16.1, 3.6, 1.1 Hz, 1 H), 3.05 (dd, J = 16.5, 13.0 Hz, 1 H), 1.64 (ddd, J = 13.3, 3.6, 2.1 Hz, 2 H), 1.24 (s, 9 H).

^{1}H{^{19}F} NMR (600 MHz, $CDCl_3$) δ: 7.73 (s, 1 H), 7.66 – 7.61 (m, 5 H), 7.18 – 7.13 (m, 4 H), 5.73 (s, 1 H), 3.50 (s, 3 H), 3.47 (s, 3 H), 3.40 (ddd, J = 16.1, 3.6, 1.3 Hz, 1 H), 3.05 (dd, J = 16.1, 13.3 Hz, 1 H), 1.64 (ddd, J = 13.4, 3.6, 2.0 Hz, 2 H), 1.24 (s, 9 H).

^{19}F NMR (565 MHz, $CDCl_3$) δ: −115.00, −115.29.

^{13}C NMR (151 MHz, $CDCl_3$) δ: 163.29 (d, J = 8.8 Hz), 161.66 (d, J = 8.4 Hz), 152.74, 152.62, 134.71 (d, J = 3.3 Hz), 134.56 (d, J = 3.3 Hz), 133.58, 133.24, 130.98 (d, J = 7.9 Hz), 130.83 (d, J = 7.8 Hz), 130.21, 129.51, 129.39, 128.08, 127.54, 127.51, 115.52 (d, J = 21.3 Hz), 115.35 (d, J = 21.2 Hz), 63.89, 62.06, 60.50, 48.29, 33.05, 28.98, 19.06.

^{13}C{^{1}H} dept-135 NMR (151 MHz, $CDCl_3$) δ: 130.86 (d, J = 8.0 Hz), 130.71 (d, J = 8.0 Hz), 130.09, 127.39, 115.40 (d, J = 21.4 Hz), 115.23 (d, J = 21.2 Hz), 63.77, 61.94, 60.38, 48.17, 28.86, 18.94.

HRMS (ESI) *m/z*:

Calcd. for $[C_{31}H_{30}F_2O_3 + Na]^+$ 511.2056 $[M + Na]^+$;
found 511.2055
$[C_{62}H_{60}F_4O_6 + Na]^+$ 999.4243 $[2\,M + Na]^+$;
found 999.4218.

Funding Information

M.M. and D.V. thank the Swiss National Science Foundation for funding (SNF Grant no. 200020 – 178808). M.M. acknowledges support from the 111 Project (Grant No. 90002 – 18011002). Open access funding enabled and organized by Project DEAL. C.W. thanks the Independent Research Fund Denmark for an international postdoctoral grant (9059 – 00003B).

Acknowledgements

We would like to thank Dr. Loïc Le Pleux and Lucius Schmid for their support during the measurement and analysis of the voltammetry data. H. Z. and L. O. thank the Kavli Institute of Nanoscience at Delft University of Technology for the infrastructure and support in MCBJ device fabrication.

Supporting Information

Supporting Information for this article is available online at https://doi.org/10.1055/a-1926-6340.

Conflict of Interest

The authors declare no conflict of interest.

References

(1) Bondyopadhyay, P. K. *Proc. IEEE* **1998**, *86*, 78.
(2) Green, J. E.; Wook Choi, J.; Boukai, A.; Bunimovich, Y.; Johnston-Halperin, E.; DeIonno, E.; Luo, Y.; Sheriff, B. A.; Xu, K.; Shik Shin, Y.; Tseng, H.-R.; Stoddart, J. F.; Heath, J. R. *Nature* **2007**, *445*, 414.
(3) Canjeevaram Balasubramanyam, R. K.; Kumar, R.; Ippolito, S. J.; Bhargava, S. K.; Periasamy, S. R.; Narayan, R.; Basak, P. *J. Phys. Chem. C* **2016**, *120*, 11313.
(4) Kano, S.; Yamada, Y.; Tanaka, K.; Majima, Y. *Appl. Phys. Lett.* **2012**, *100*, 053101.
(5) Park, H.; Park, J.; Lim, A. K. L.; Anderson, E. H.; Alivisatos, A. P.; McEuen, P. L. *Nature* **2000**, *407*, 57.
(6) Park, J.; Pasupathy, A. N.; Goldsmith, J. I.; Chang, C.; Yaish, Y.; Petta, J. R.; Rinkoski, M.; Sethna, J. P.; Abruña, H. D.; McEuen, P. L.; Ralph, D. C. *Nature* **2002**, *417*, 722.
(7) Kubatkin, S.; Danilov, A.; Hjort, M.; Cornil, J.; Brédas, J.-L.; Stuhr-Hansen, N.; Hedegård, P.; Bjørnholm, T. Nature **2003**, *425*, 698.
(8) Elbing, M.; Ochs, R.; Koentopp, M.; Fischer, M.; von Hänisch, C.; Weigend, F.; Evers, F.; Weber, H. B.; Mayor, M. *Proc. Natl. Acad. Sci. U. S. A.* **2005**, *102*, 8815.
(9) Díez-Pérez, I.; Hihath, J.; Lee, Y.; Yu, L.; Adamska, L.; Kozhushner, M. A.; Oleynik, I. I.; Tao, N. *Nat. Chem.* **2009**, *1*, 635.
(10) Blum, A. S.; Kushmerick, J. G.; Long, D. P.; Patterson, C. H.; Yang, J. C.; Henderson, J. C.; Yao, Y.; Tour, J. M.; Shashidhar, R.; Ratna, B. R. *Nat. Mater.* **2005**, *4*, 167.
(11) Quek, S. Y.; Kamenetska, M.; Steigerwald, M. L.; Choi, H. J.; Louie, S. G.; Hybertsen, M. S.; Neaton, J. B.; Venkataraman, L. *Nat. Nanotechnol.* **2009**, *4*, 230.
(12) Pease, A. R.; Jeppesen, J. O.; Stoddart, J. F.; Luo, Y.; Collier, C. P.; Heath, J. R. *Acc. Chem. Res.* **2001**, *34*, 433.
(13) Molen, S. J. van der; Liljeroth, P. *J. Phys.: Condens. Matter* **2010**, *22*, 133001.
(14) Li, Z.; Smeu, M.; Afsari, S.; Xing, Y.; Ratner, M. A.; Borguet, E. *Angew. Chem. Int. Ed.* **2014**, *53*, 1098.
(15) Akimov, A. V.; Kolomeisky, A. B. *J. Phys. Chem. C* **2012**, *116*, 22595.
(16) Simão, C.; Mas-Torrent, M.; Casado-Montenegro, J.; Otón, F.; Veciana, J.; Rovira, C. *J. Am. Chem. Soc.* **2011**, *133*, 13256.
(17) Li, H.; Xu, Q.; Li, N.; Sun, R.; Ge, J.; Lu, J.; Gu, H.; Yan, F. *J. Am. Chem. Soc.* **2010**, *132*, 5542.
(18) Raymo, F. M.; Giordani, S.; White, A. J. P.; Williams, D. J. *J. Org. Chem.* **2003**, *68*, 4158.
(19) Irie, M. *Chem. Rev.* **2000**, *100*, 1685.
(20) Weibel, N.; Grunder, S.; Mayor, M. *Org. Biomol. Chem.* **2007**, *5*, 2343.
(21) Stoddart, J. F.; Colquhoun, H. M. *Tetrahedron* **2008**, *64*, 8231.
(22) Le Pleux, L.; Kapatsina, E.; Hildesheim, J.; Häussinger, D.; Mayor, M. *Eur. J. Org. Chem.* **2017**, *2017*, 3165.
(23) Yin, X.; Zang, Y.; Zhu, L.; Low, J. Z.; Liu, Z.-F.; Cui, J.; Neaton, J. B.; Venkataraman, L.; Campos, L. M. *Sci. Adv.* **2017**, *3*, eaao2615.
(24) Wu, S. W.; Ogawa, N.; Nazin, G. V.; Ho, W. *J. Phys. Chem. C* **2008**, *112*, 5241.
(25) Osorio, E. A.; O'Neill, K.; Wegewijs, M.; Stuhr-Hansen, N.; Paaske, J.; Bjørnholm, T.; van der Zant, H. S. J. *Nano Lett.* **2007**, *7*, 3336.
(26) Qiu, X. H.; Nazin, G. V.; Ho, W. *Phys. Rev. Lett.* **2004**, *93*, 196806.
(27) Thijssen, J. M.; Van der Zant, H. S. J. *Phys. Status Solidi B* **2008**, *245*, 1455.
(28) Tao, N. J. *Phys. Rev. Lett.* **1996**, *76*, 4066.
(29) Brandl, T.; El Abbassi, M.; Stefani, D.; Frisenda, R.; Harzmann, G. D.; van der Zant, H. S. J.; Mayor, M. *Eur. J. Org. Chem.* **2019**, *2019*, 5334.
(30) Dulić, D.; Kudernac, T.; Pužys, A.; Feringa, B. L.; van Wees, B. J. *Adv. Mater.* **2007**, *19*, 2898.
(31) Gütlich, P.; Hauser, A.; Spiering, H. *Angew. Chem. Int. Ed.* **1994**, *33*, 2024.
(32) Šalitroš, I.; Madhu, N. T.; Boča, R.; Pavlik, J.; Ruben, M. *Monatsh. Chem.* **2009**, *140*, 695.
(33) Gamez, P.; Costa, J. S.; Quesada, M.; Aromí, G. *Dalton Trans.* **2009**, 7845.
(34) Frisenda, R.; Harzmann, G. D.; Celis Gil, J. A.; Thijssen, J. M.; Mayor, M.; van der Zant, H. S. J. *Nano Lett.* **2016**, *16*, 4733.
(35) Xu, B.; Tao, N. J. *Science* **2003**, *301*, 1221.
(36) Hybertsen, M. S.; Venkataraman, L. Acc. Chem. Res. **2016**, *49*, 452.
(37) Gehring, P.; Thijssen, J. M.; van der Zant, H. S. J. *Nat. Rev. Phys.* **2019**, *1*, 381.
(38) van Ruitenbeek, J. M.; Alvarez, A.; Piñeyro, I.; Grahmann, C.; Joyez, P.; Devoret, M. H.; Esteve, D.; Urbina, C. *Rev. Sci. Instrum.* **1996**, *67*, 108.
(39) Wang, L.; Wang, L.; Zhang, L.; Xiang, D. *Molecular-Scale Electronics: Current Status and Perspectives*; In *Topics in Current Chemistry Collections*; Guo, X.; Springer International Publishing: Cham, **2019**; 45.
(40) Dulić, D.; van der Molen, S. J.; Kudernac, T.; Jonkman, H. T.; de Jong, J. J. D.; Bowden, T. N.; van Esch, J.; Feringa, B. L.; van Wees, B. J. *Phys. Rev. Lett.* **2003**, *91*, 207402.
(41) Whalley, A. C.; Steigerwald, M. L.; Guo, X.; Nuckolls, C. *J. Am. Chem. Soc.* **2007**, *129*, 12590.
(42) Zhou, J.; Wang, K.; Xu, B.; Dubi, Y. *J. Am. Chem. Soc.* **2018**, *140*, 70.
(43) Cao, Y.; Dong, S.; Liu, S.; Liu, Z.; Guo, X. *Angew. Chem. Int. Ed.* **2013**, *52*, 3906.
(44) Meng, L.; Xin, N.; Hu, C.; Wang, J.; Gui, B.; Shi, J.; Wang, C.; Shen, C.; Zhang, G.; Guo, H.; Meng, S.; Guo, X. *Nat. Commun.* **2019**, *10*, 1450.
(45) Roldan, D.; Kaliginedi, V.; Cobo, S.; Kolivoska, V.; Bucher, C.; Hong, W.; Royal, G.; Wandlowski, T. *J. Am. Chem. Soc.* **2013**, *135*, 5974.
(46) Li, Y.; Baghernejad, M.; Qusiy, A.-G.; Zsolt Manrique, D.; Zhang, G.; Hamill, J.; Fu, Y.; Broekmann, P.; Hong, W.; Wandlowski, T.; Zhang, D.; Lambert, C. *Angew. Chem.* **2015**, *127*, 13790.

(47) Hatanaka, K.; Morita, Y.; Ohba, T.; Yamaguchi, K.; Takui, T.; Kinoshita, M.; Nakasuji, K. *Tetrahedron Lett.* **1996**, *37*, 873.
(48) Hatanaka, K.; Morita, Y.; Ohba, T.; Yamaguchi, K.; Takui, T.; Kinoshita, M.; Nakasuji, K. *Tetrahedron Lett.* **1996**, *37*, 877.
(49) Morita, Y.; Ohba, T.; Haneda, N.; Maki, S.; Kawai, J.; Hatanaka, K.; Sato, K.; Shiomi, D.; Takui, T.; Nakasuji, K. *J. Am. Chem. Soc.* **2000**, *122*, 4825.
(50) Morita, Y.; Maki, S.; Fukui, K.; Ohba, T.; Kawai, J.; Sato, K.; Shiomi, D.; Takui, T.; Nakasuji, K. *Org. Lett.* **2001**, *3*, 3099.
(51) Nishida, S.; Kawai, J.; Moriguchi, M.; Ohba, T.; Haneda, N.; Fukui, K.; Fuyuhiro, A.; Shiomi, D.; Sato, K.; Takui, T.; Nakasuji, K.; Morita, Y. *Chem. Eur. J.* **2013**, *19*, 11904.
(52) Nishida, S.; Kariyazono, K.; Yamanaka, A.; Fukui, K.; Sato, K.; Takui, T.; Nakasuji, K.; Morita, Y. *Chem. Asian J.* **2011**, *6*, 1188.
(53) Morita, Y.; Kawai, J.; Haneda, N.; Nishida, S.; Fukui, K.; Nakazawa, S.; Shiomi, D.; Sato, K.; Takui, T.; Kawakami, T.; Yamaguchi, K.; Nakasuji, K. *Tetrahedron Lett.* **2001**, *42*, 7991.
(54) Morita, Y.; Nishida, S.; Kawai, J.; Fukui, K.; Nakazawa, S.; Sato, K.; Shiomi, D.; Takui, T.; Nakasuji, K. *Org. Lett.* **2002**, *4*, 1985.
(55) Nishida, S.; Morita, Y.; Fukui, K.; Sato, K.; Shiomi, D.; Takui, T.; Nakasuji, K. *Angew. Chem. Int. Ed.* **2005**, *44*, 7277.
(56) Pyurbeeva, E.; Hsu, C.; Vogel, D.; Wegeberg, C.; Mayor, M.; van der Zant, H.; Mol, J. A.; Gehring, P. *Nano Lett.* **2021**, *21*, 9715.
(57) Hsu, C.; Costi, T. A.; Vogel, D.; Wegeberg, C.; Mayor, M.; van der Zant, H. S. J.; Gehring, P. *Phys. Rev. Lett.* **2022**, *128*, 147701.
(58) Goto, K.; Kubo, T.; Yamamoto, K.; Nakasuji, K.; Sato, K.; Shiomi, D.; Takui, T.; Kubota, M.; Kobayashi, T.; Yakusi, K.; Ouyang, J. *J. Am. Chem. Soc.* **1999**, *121*, 1619.
(59) Park, M. S.; Kim, G.; Won, H.; Han, J. W.; Oh, C. H. *Bull. Korean Chem. Soc.* **2020**, *41*, 88.
(60) Storch, J.; Bernard, M.; Sýkora, J.; Karban, J.; Čermák, J. Eur. J. Org. Chem. **2013**, *2013*, 260.
(61) Hwang, J. P.; Surya Prakash, G. K.; Olah, G. A. *Tetrahedron* **2000**, *56*, 7199.
(62) Schnürch, M.; Spina, M.; Khan, A. F.; Mihovilovic, M. D.; Stanetty, P. *Chem. Soc. Rev.* **2007**, *36*, 1046.
(63) Tutino, F.; Papeo, G.; Quartieri, F. *J. Heterocycl. Chem.* **2010**, *47*, 112.
(64) Subramanian, L. R.; Martínez, A. G.; Hanack, M.; Surya Prakash, G. K.; Hu, J. *Encyclopedia of Reagents for Organic Synthesis*; John Wiley & Sons, Ltd: New York, **2006**.
(65) Akhlaghinia, B.; Pourali, A.-R.; Rahmani, M. *Synth. Commun.* **2012**, *42*, 1184.
(66) Chikkanna, D.; McCarthy, C.; Moebitz, H.; Pandit, C.; Sistla, R.; Subramanya, H. US 20090275606 (A1) **2009**.
(67) Qiu, D.; Jin, L.; Zheng, Z.; Meng, H.; Mo, F.; Wang, X.; Zhang, Y.; Wang, J. *J. Org. Chem.* **2013**, *78*, 1923.
(68) Xue, C.-B.; Li, Y.-L.; Geng, H.; Pan, J.; Wang, A.; Zhang, K.; Yao, W.; Zhang, F.; Zhuo, J. US 20140200227 (A1) **2014**.
(69) Burger, M.; Nishiguchi, G.; Rico, A.; Simmons, R. L.; Tamez, J. V.; Tanner, H.; Wan, L. WO2014033631 (A1), **2014**.
(70) Hinkes, S. P. A.; Klein, C. D. P. *Org. Lett.* **2019**, *21*, 3048.
(71) Mukhopadhyay, T.; Seebach, D. *Helv. Chim. Acta* **1982**, *65*, 385.
(72) Wilmarth, W. K.; Schwartz, N. *J. Am. Chem. Soc.* **1955**, *77*, 4543.
(73) Morita, Y.; Nishida, S.; Kawai, J.; Takui, T.; Nakasuji, K. *Pure Appl. Chem.* **2008**, *80*, 507.
(74) Schweiger, A.; Jeschke, G. *Principles of Pulse Electron Paramagnetic Resonance*; Oxford University Press: Oxford, New York, **2001**.
(75) Giuffredi, G. T.; Gouverneur, V.; Bernet, B. *Angew. Chem. Int. Ed.* **2013**, *52*, 10524.
(76) Paul, A.; Borrelli, R.; Bouyanfif, H.; Gottis, S.; Sauvage, F. *ACS Omega* **2019**, *4*, 14780.
(77) Willems, R. E. M.; Weijtens, C. H. L.; de Vries, X.; Coehoorn, R.; Janssen, R. A. J. *Adv. Energy Mater.* **2019**, *9*, 1803677.
(78) Tessensohn, M. E.; Webster, R. D. *Electrochem. Commun.* **2016**, *62*, 38.
(79) Hui, Y.; Chng, E. L. K.; Chng, C. Y. L.; Poh, H. L.; Webster, R. D. *J. Am. Chem. Soc.* **2009**, *131*, 1523.
(80) Huber, R.; González, M. T.; Wu, S.; Langer, M.; Grunder, S.; Horhoiu, V.; Mayor, M.; Bryce, M. R.; Wang, C.; Jitchati, R.; Schönenberger, C.; Calame, M. *J. Am. Chem. Soc.* **2008**, *130*, 1080.
(81) Cabosart, D.; El Abbassi, M.; Stefani, D.; Frisenda, R.; Calame, M.; van der Zant, H. S. J.; Perrin, M. L. *Appl. Phys. Lett.* **2019**, *114*, 143102.
(82) Untiedt, C.; Yanson, A. I.; Grande, R.; Rubio-Bollinger, G.; Agraït, N.; Vieira, S.; van Ruitenbeek, J. M. *Phys. Rev. B: Condes. Matter* **2002**, *66*, 085418.
(83) Hong, W.; Manrique, D. Z.; Moreno-García, P.; Gulcur, M.; Mishchenko, A.; Lambert, C. J.; Bryce, M. R.; Wandlowski, T. *J. Am. Chem. Soc.* **2012**, *134*, 2292.
(84) O'Driscoll, J. L.; Bryce, R. M. *Nanoscale* **2021**, *13*, 10668.
(85) Leary, E.; Zotti, L. A.; Miguel, D.; Márquez, I. R.; Palomino-Ruiz, L.; Cuerva, J. M.; Rubio-Bollinger, G.; González, M. T.; Agrait, N. *J. Phys. Chem. C* **2018**, *122*, 3211.
(86) Hindenberg, P.; Busch, M.; Paul, A.; Bernhardt, M.; Gemessy, P.; Rominger, F.; Romero-Nieto, C. *Angew. Chem. Int. Ed.* **2018**, *57*, 15157.
(87) Tate, D. J.; Abdelbasit, M.; Kilner, C. A.; Shepherd, H. J.; Warriner, S. L.; Bushby, R. J. *Tetrahedron* **2014**, *70*, 67.
(88) Xu, Y.; Cong, T.; Liu, P.; Sun, P. *Org. Biomol. Chem.* **2015**, *13*, 9742.
(89) Kloosterziel, H.; Backer, H. J. *Recl. Trav. Chim. Pays-Bas* **1953**, *72*, 655.
(90) Miao, R.-G.; Qi, X.; Wu, X.-F. *Eur. J. Org. Chem.* **2021**, *2021*, 5219.